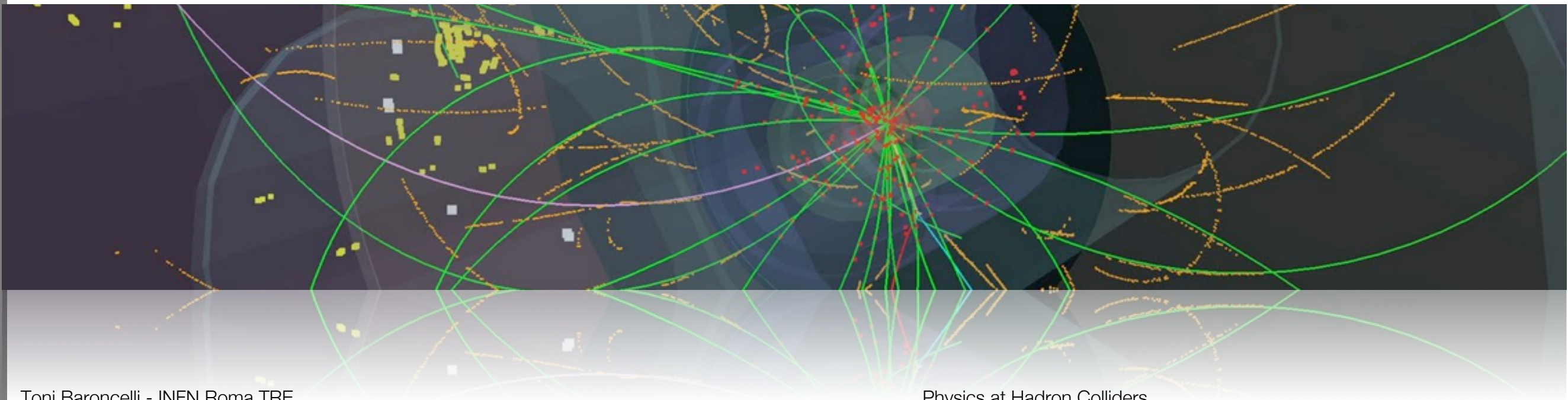# Lecture 4 Cross Section Measurements
Ingredients to a Cross Section

Mostly Deep Inelastic Scattering

Prerequisites and Reminders ...

Natural Units
Four-Vector Kinematics
Lorentz Transformation
Lorentz Boost
Lorentz Invariance
Rapidity etc.
Invariant Mass
CMS-Energy

Particle Decays
Cross Section
Matrix Element
Phase Space
Feynman Diagrams
Mandelstam Variables

Parton Distributions
Bjorken-x

...

$$\hbar = 1, \ c = 1$$

$$\hbar c = 197.3 \ \text{MeV fm}$$
$$(\hbar c)^2 = 0.3894 \ \text{GeV}^2 \ \text{mb}$$

$$p = (E, \vec{p})$$

$$p^2 = E^2 - \vec{p}^2 = m^2$$

$$\beta = p/E, \ \gamma = E/m$$

$$p_1 \cdot p_2 = E_1 E_2 - \vec{p}_1 \cdot \vec{p}_2$$

4-vector scalar product
Lorentz invariant

→ All quantities like cross sections etc.
should be in terms of scalar products of 4-vectors ...

Prerequisites and Reminders ...

Natural Units
Four-Vector Kinematics
Lorentz Transformation
Lorentz Boost
Lorentz Invariance
Rapidity etc.
Invariant Mass
CMS-Energy

Particle Decays
Cross Section
Matrix Element
Phase Space
Feynman Diagrams
Mandelstam Variables

Parton Distributions
Bjorken-x

...

$$p = (E, \vec{p})$$

Particle momentum as seen
in laboratory frame ...

$$p^* = (E^*, \vec{p}^{\,*})$$

Particle momentum as viewed from a
frame moving with velocity β_f ...

Lorentz Transformation:

$$E^* = \gamma_f \cdot E - \gamma_f \beta_f \cdot p_{\parallel}$$
$$p_{\parallel}^* = \gamma_f \cdot p_{\parallel} - \gamma_f \beta_f \cdot E$$
$$p_T^* = p_T$$

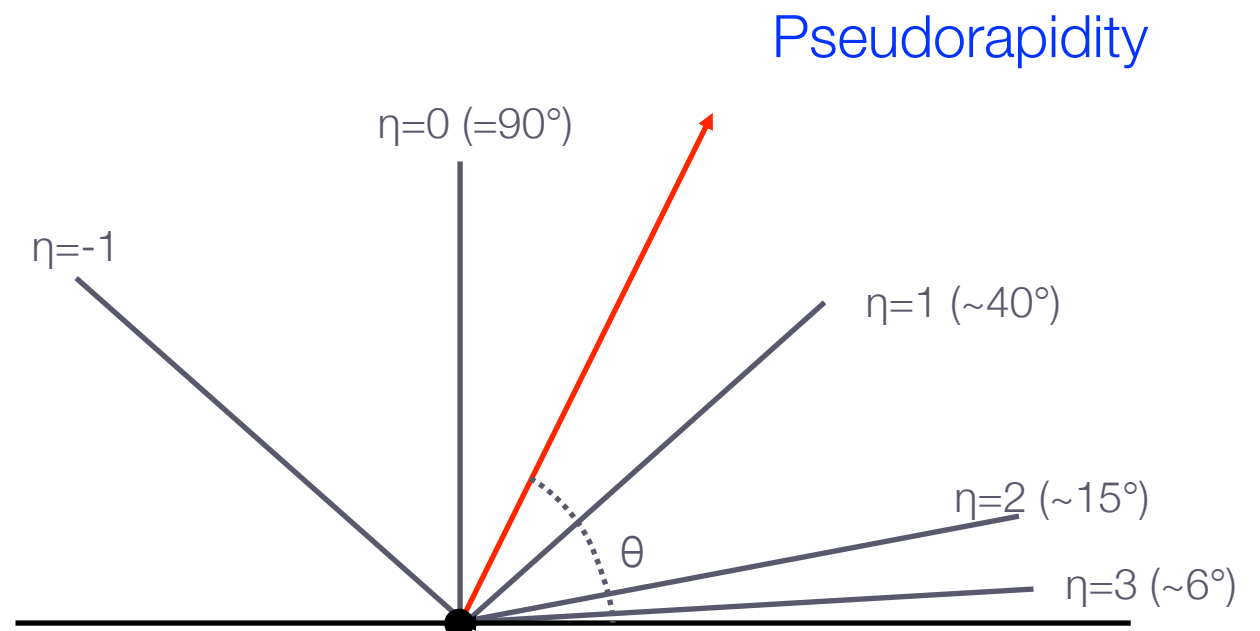with $\quad \gamma_f = (1 - \beta_f^2)^{-\frac{1}{2}}$

Prerequisites and Reminders ...

Natural Units
Four-Vector Kinematics
Lorentz Transformation
Lorentz Boost
Lorentz Invariance
Rapidity etc.
Invariant Mass
CMS-Energy

Particle Decays
Cross Section
Matrix Element
Phase Space
Feynman Diagrams
Mandelstam Variables

Parton Distributions
Bjorken-x

...

p_T

$x_1 p$ $x_2 p$ Proton

$\sqrt{\hat{s}}$

Proton

Schematic
proton-proton scattering
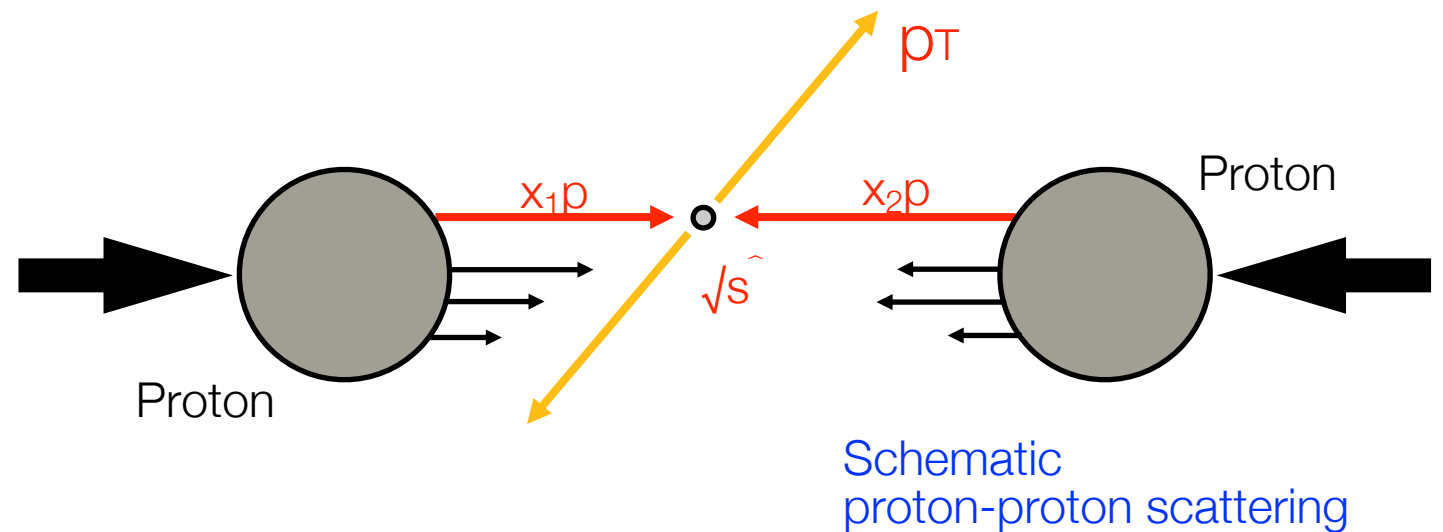
Relevant kinematic variables:

- Transverse momentum: p_T
- Rapidity: $y = \frac{1}{2} \cdot \ln (E-p_z)/(E+p_z)$
- Pseudorapidity: $\eta = -\ln \tan \frac{1}{2}\theta$
- Azimuthal angle: ϕ

Pseudorapidity

$\eta=0$ (=90°)

$\eta=-1$

$\eta=1$ (~40°)

$\eta=2$ (~15°)

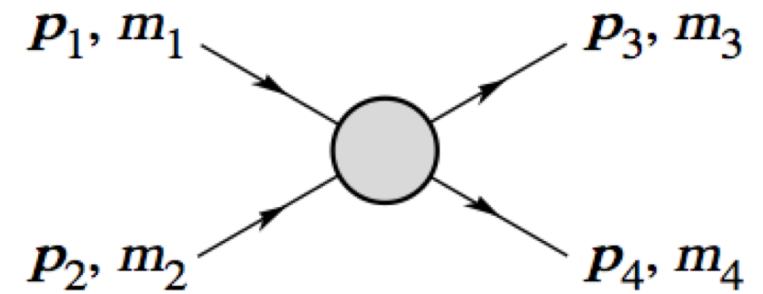θ

$\eta=3$ (~6°)

Prerequisites and Reminders ...

Natural Units
Four-Vector Kinematics
Lorentz Transformation
Lorentz Boost
Lorentz Invariance
Rapidity etc.
Invariant Mass
CMS-Energy

Particle Decays
Cross Section
Matrix Element
Phase Space
Feynman Diagrams
Mandelstam Variables

Parton Distributions
Bjorken-x

...

Invariant Mass:

$$M^2 = (p_1 + p_2)^2$$
$$= (E_1 + E_2)^2 - (\vec{p}_1 + \vec{p}_2)^2$$
$$= m_1^2 + m_2^2 + 2E_1 E_2 (1 - \vec{\beta}_1 \vec{\beta}_2)$$

Center-of-mass Energy:

$$E_{\mathrm{cm}} = \left[(E_1 + E_2)^2 - (\vec{p}_1 + \vec{p}_2)^2\right]^{\frac{1}{2}}$$

Particle 2 at rest:

$$E_{\mathrm{cm}} = \left[m_1^2 + m_2^2 + 2E_1 m_2\right]^{\frac{1}{2}}$$

Particle Collider:

$$[E_1 = E_2;\ \vec{p}_1 = -\vec{p}_2;\ m_1 = m_2 \approx 0]$$

$$E_{\mathrm{cm}} = 2E$$

Prerequisites and Reminders ...

Natural Units
Four-Vector Kinematics
Lorentz Transformation
Lorentz Boost
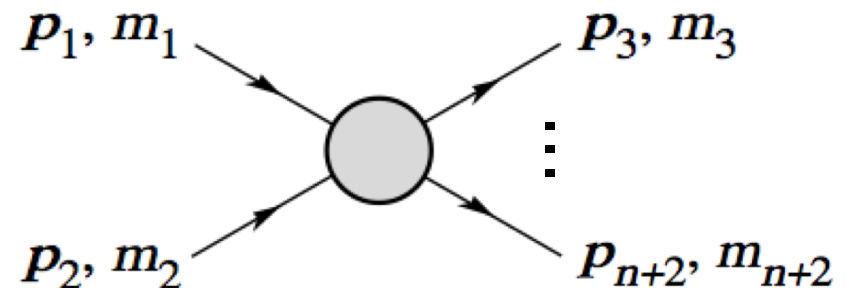Lorentz Invariance
Rapidity etc.
Invariant Mass
CMS-Energy

Cross Section
Particle Decays
Matrix Element
Phase Space
Feynman Diagrams
Mandelstam Variables

Parton Distributions
Bjorken-x

...

$$p_1, m_1 \qquad p_3, m_3$$

$$p_2, m_2 \qquad p_{n+2}, m_{n+2}$$

Differential
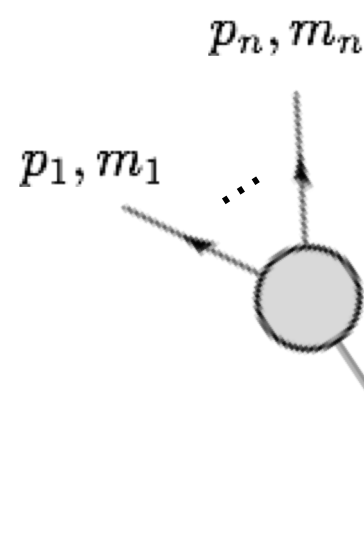Cross Section:

Matrix element

$$d\sigma = \frac{(2\pi)^4 |\mathcal{M}|^2}{4\sqrt{(p_1 \cdot p_2)^2 - m_1^2 m_2^2}}$$

$$\times \quad d\Phi_n(p_1 + p_2; \; p_3, \ldots, p_{n+2})$$

n-body
phase space

$$d\Phi_n = \ldots$$
$$\ldots = \delta^4\left(P - \sum_{i=1}^{n} p_i\right) \prod_{i=1}^{n} \frac{d^3 p_i}{(2\pi)^3 2E_i}$$

$$p_n, m_n \qquad \text{Partial}$$
Decay Rate:

with $\quad P = p_1 + p_2$

$$p_1, m_1$$

$$d\Gamma = \frac{(2\pi)^4}{2M} |\mathcal{M}|^2$$

$$\times \quad d\Phi_n(P; \; p_1, \ldots, p_n)$$

$$P, M$$

Toni Baroncelli - INFN Roma TRE

Physics at Hadron Colliders

Prerequisites and Reminders ...

Natural Units
Four-Vector Kinematics
Lorentz Transformation
Lorentz Boost
Lorentz Invariance
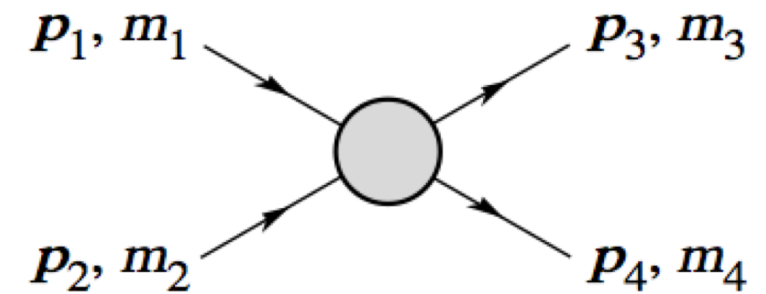Rapidity etc.
Invariant Mass
CMS-Energy

Particle Decays
Cross Section
Matrix Element
Phase Space
Feynman Diagrams
Mandelstam Variables
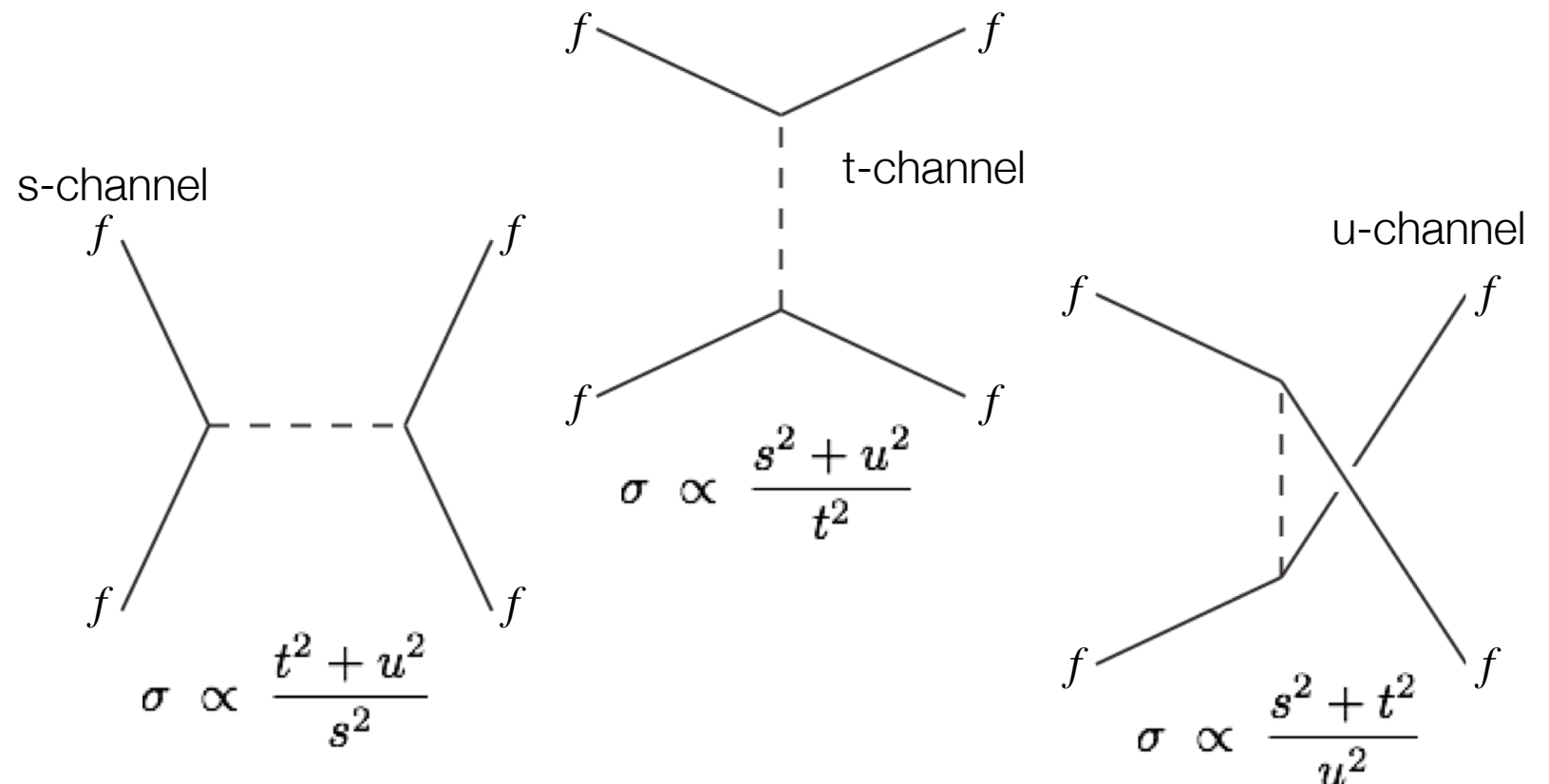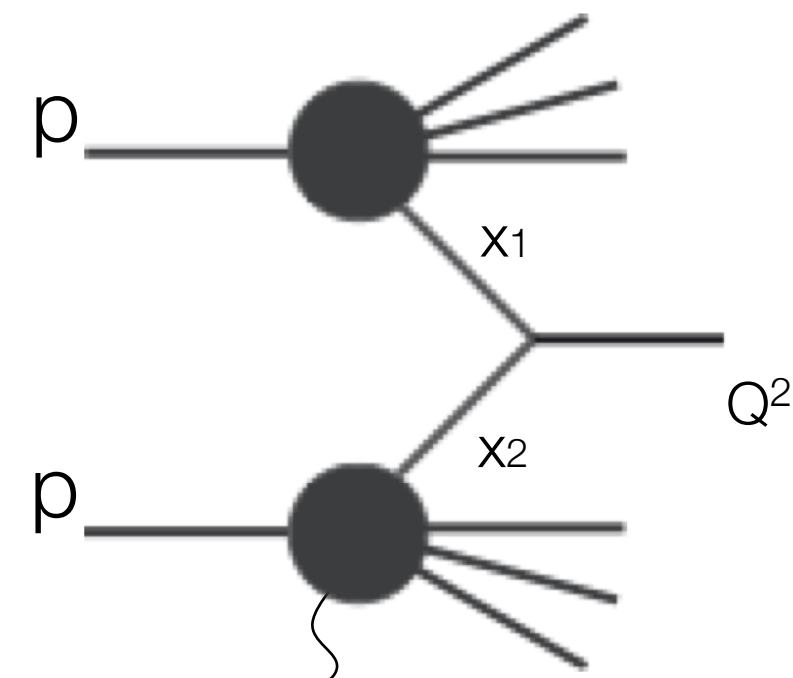
Parton Distributions
Bjorken-x
...

p_1, m_1 p_3, m_3

p_2, m_2 p_4, m_4

Mandelstam variables:

$$s = (p_1 + p_2)^2 = (p_3 + p_4)^2$$
$$t = (p_1 - p_3)^2 = (p_2 - p_4)^2$$
$$u = (p_1 - p_4)^2 = (p_2 - p_3)^2$$

s-channel

$$\sigma \propto \frac{t^2 + u^2}{s^2}$$

t-channel

$$\sigma \propto \frac{s^2 + u^2}{t^2}$$

u-channel

$$\sigma \propto \frac{s^2 + t^2}{u^2}$$

Prerequisites and Reminders ...

Natural Units
Four-Vector Kinematics
Lorentz Transformation
Lorentz Boost
Lorentz Invariance
Rapidity etc.
Invariant Mass
CMS-Energy

Particle Decays
Cross Section
Matrix Element
Phase Space
Feynman Diagrams
Mandelstam Variables

Parton Distributions
Bjorken-x

...

Proton-Proton
Cross Section:

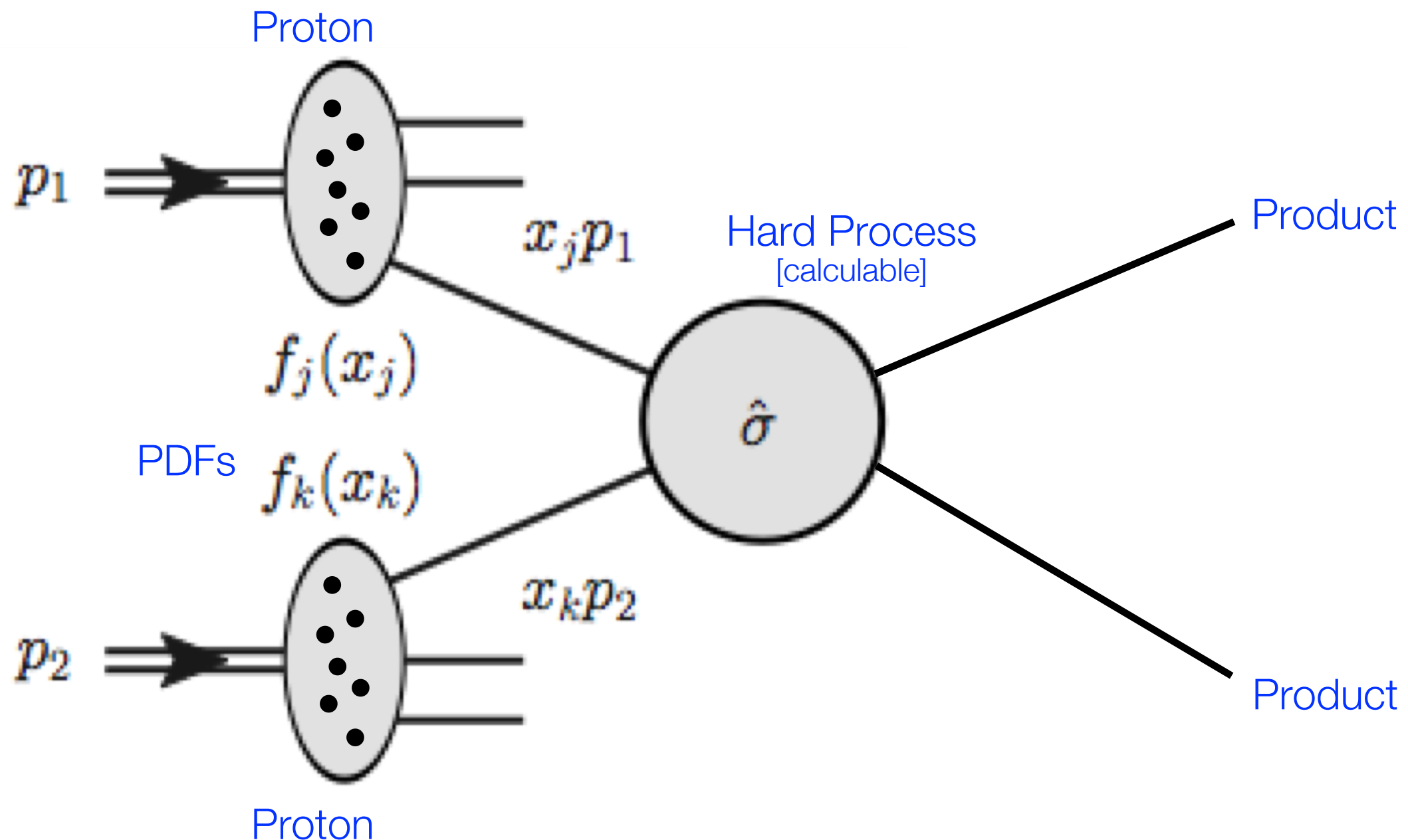$$\sigma = \sum_{ij} \int dx_1 dx_2 \; f_i(x_1, Q^2) \, f_j(x, Q^2) \, \hat{\sigma}(Q^2)$$

Parton content:
$f(x,Q^2) = q(x,Q^2)$ or $g(x,Q^2)$

$x_{1,2}$: Bjorken-x
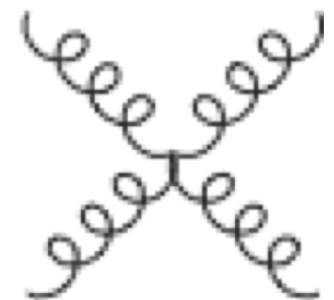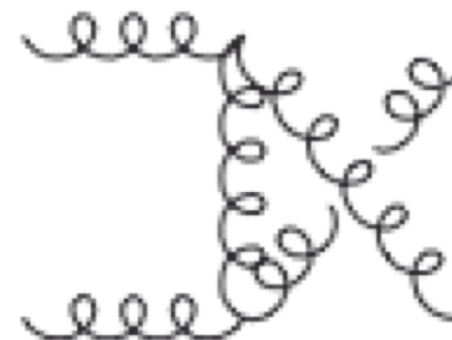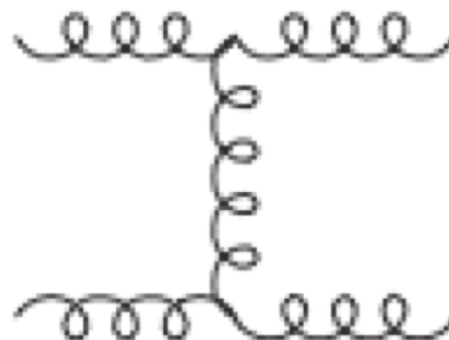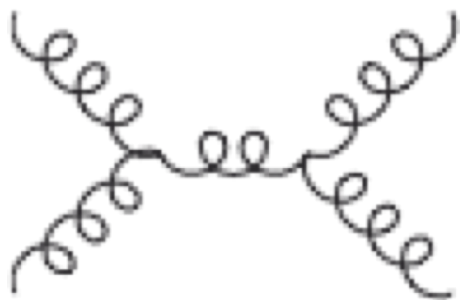fractional momentum of parton
involved in hard process

Q^2 : scale; spatial resolution
invariant parton-parton mass

f : Parton Distribution function
measured e.g. at HERA ...

Proton-Proton Scattering @ LHC

Some Hard Processes ...
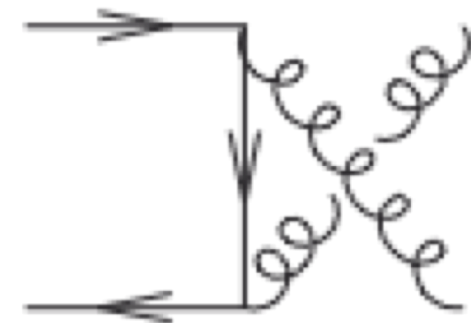
QCD Matrix Elements

Hard scattering!

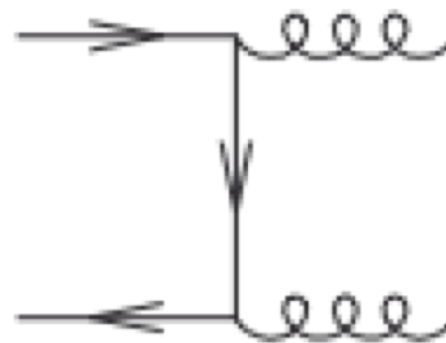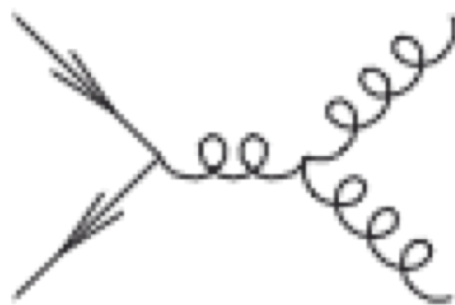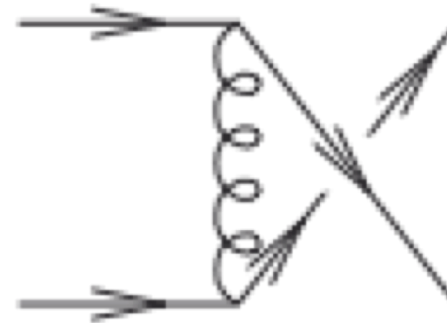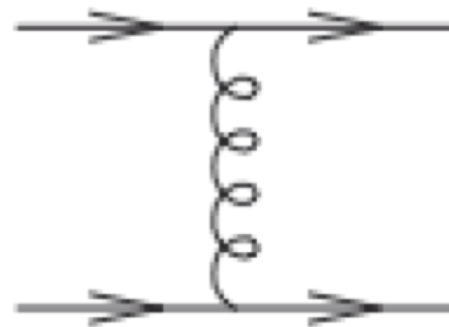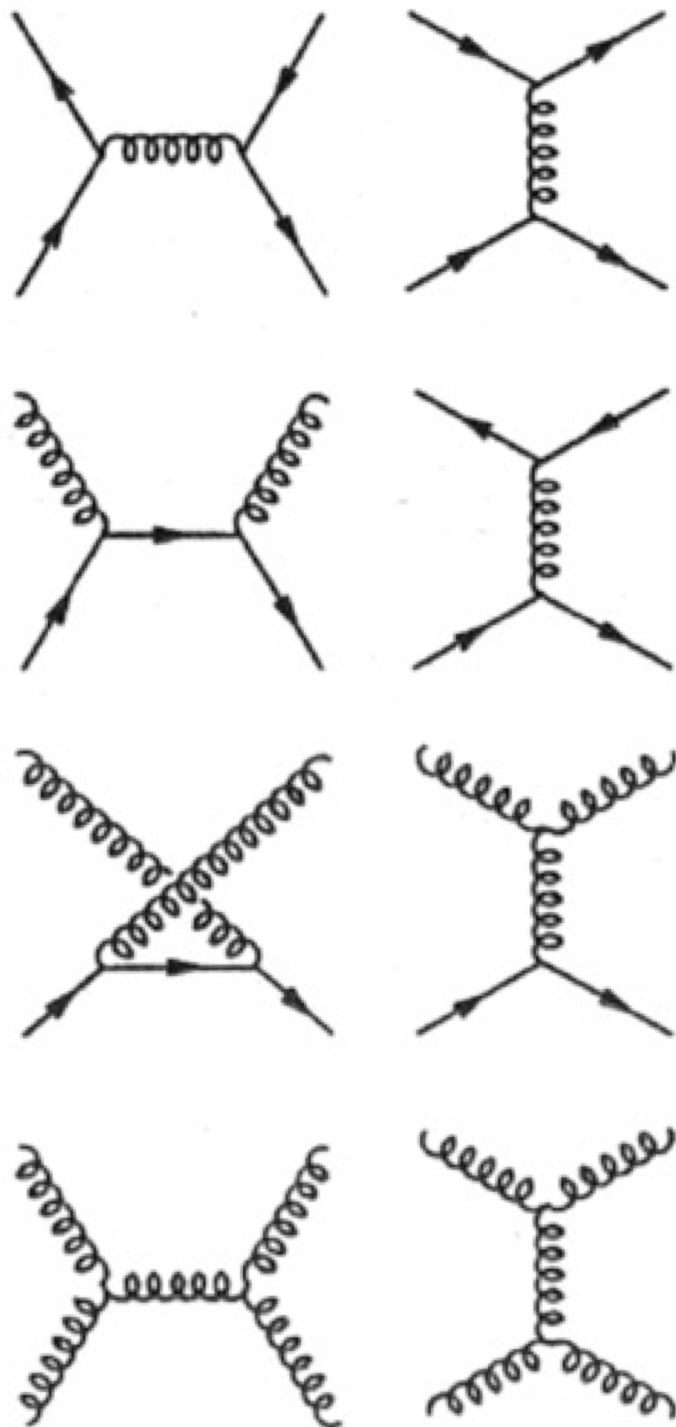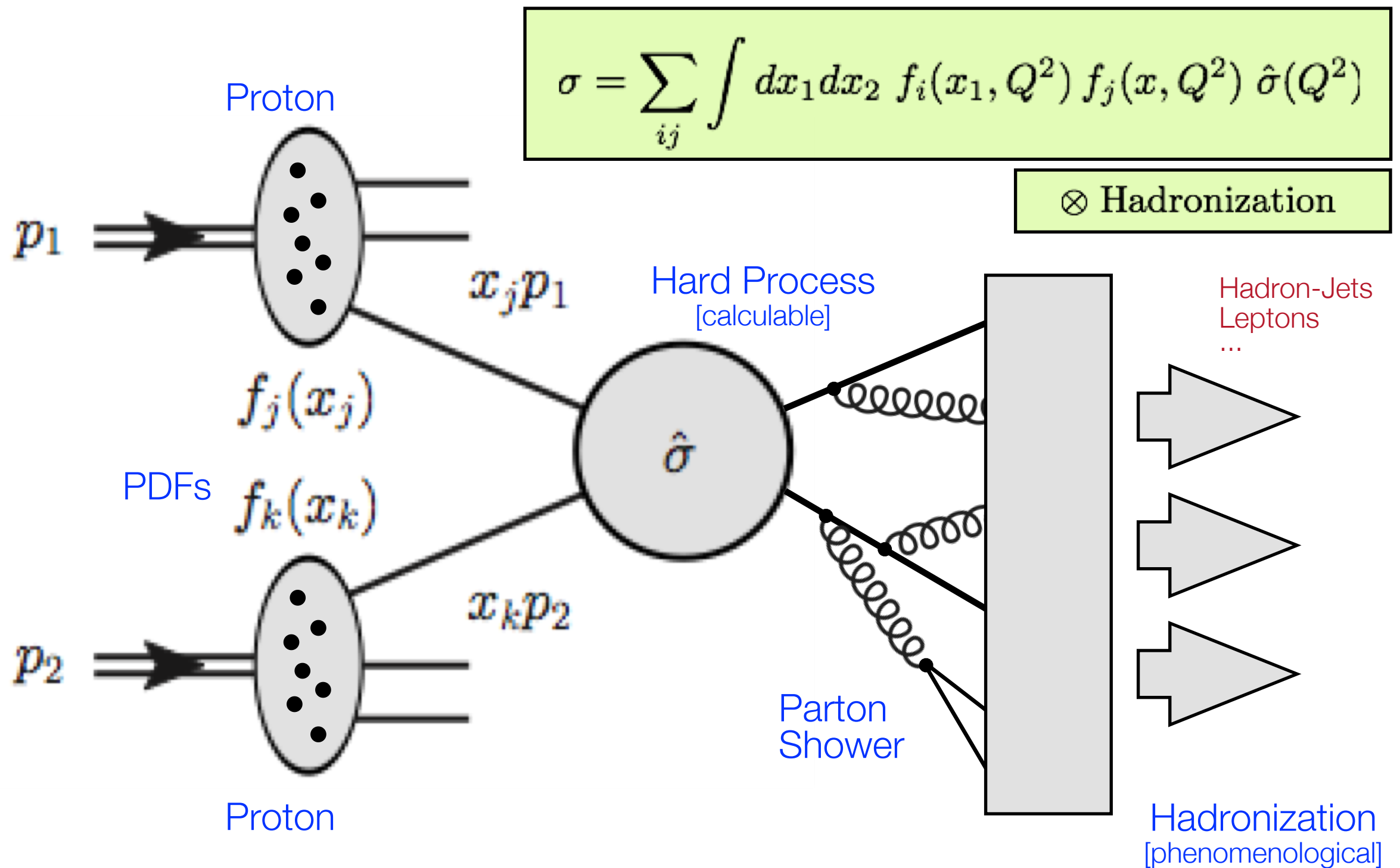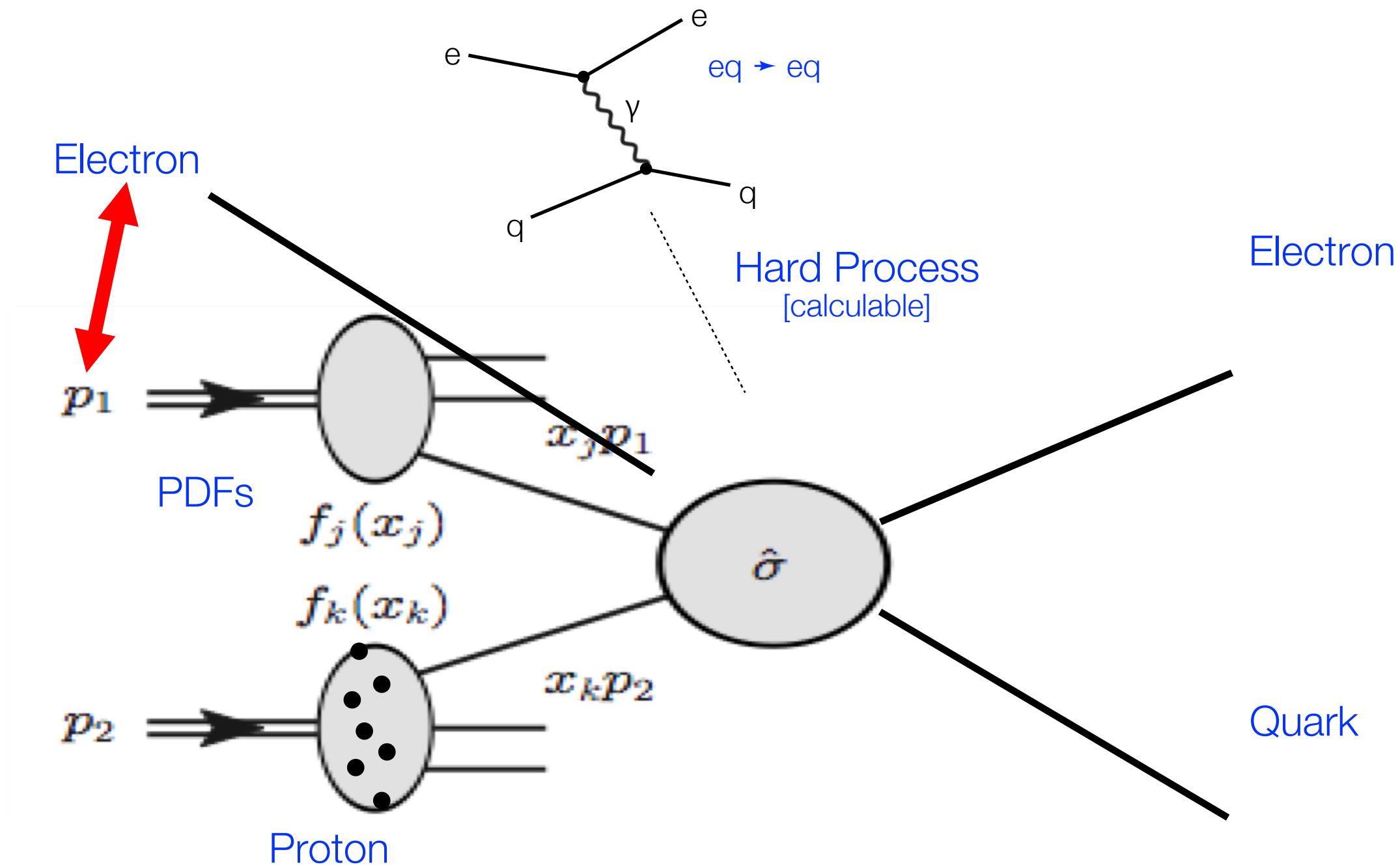| Subprocess	$|\mathcal{M}|^2/g_s^4$	$|\mathcal{M}(90°)|^2/g_s^4$
$\begin{aligned} qq' &\to qq' \\ q\bar{q}' &\to q\bar{q}' \end{aligned}$	$\dfrac{4}{9}\dfrac{\hat{s}^2+\hat{u}^2}{\hat{t}^2}$	2.2
$qq \to qq$	$\dfrac{4}{9}\left(\dfrac{\hat{s}^2+\hat{u}^2}{\hat{t}^2}+\dfrac{\hat{s}^2+\hat{t}^2}{\hat{u}^2}\right)-\dfrac{8}{27}\dfrac{\hat{s}^2}{\hat{u}\hat{t}}$	3.3
$q\bar{q} \to q'\bar{q}'$	$\dfrac{4}{9}\dfrac{\hat{t}^2+\hat{u}^2}{\hat{s}^2}$	0.2
$q\bar{q} \to q\bar{q}$	$\dfrac{4}{9}\left(\dfrac{\hat{s}^2+\hat{u}^2}{\hat{t}^2}+\dfrac{\hat{t}^2+\hat{u}^2}{\hat{s}^2}\right)-\dfrac{8}{27}\dfrac{\hat{u}^2}{\hat{s}\hat{t}}$	2.6
$q\bar{q} \to gg$	$\dfrac{32}{27}\dfrac{\hat{u}^2+\hat{t}^2}{\hat{u}\hat{t}}-\dfrac{8}{3}\dfrac{\hat{u}^2+\hat{t}^2}{\hat{s}^2}$	1.0
$gg \to q\bar{q}$	$\dfrac{1}{6}\dfrac{\hat{u}^2+\hat{t}^2}{\hat{u}\hat{t}}-\dfrac{3}{8}\dfrac{\hat{u}^2+\hat{t}^2}{\hat{s}^2}$	0.1
$qg \to qg$	$\dfrac{\hat{s}^2+\hat{u}^2}{\hat{t}^2}-\dfrac{4}{9}\dfrac{\hat{s}^2+\hat{u}^2}{\hat{u}\hat{s}}$	6.1
$gg \to gg$	$\dfrac{9}{4}\left(\dfrac{\hat{s}^2+\hat{u}^2}{\hat{t}^2}+\dfrac{\hat{s}^2+\hat{t}^2}{\hat{u}^2}+\dfrac{\hat{u}^2+\hat{t}^2}{\hat{s}^2}+3\right)$	30.4

$$\sigma = \sum_{ij} \int dx_1 dx_2 \; f_i(x_1, Q^2) \, f_j(x, Q^2) \, \hat{\sigma}(Q^2)$$

$\otimes$ Hadronization

Proton

p_1

$x_j p_1$

$f_j(x_j)$

PDFs $f_k(x_k)$

$x_k p_2$

p_2

Proton

Hard Process
[calculable]

$\hat{\sigma}$

Parton
Shower

Hadron-Jets
Leptons
...

Hadronization
[phenomenological]

Electron-Proton Scattering

eq ➤ eq

Electron

p_1

PDFs

$f_j(x_j)$

$x_j p_1$

Hard Process
[calculable]

e

e

γ

q

q

Electron

$\hat{\sigma}$

$f_k(x_k)$

$x_k p_2$

p_2

Quark

Proton

Electron-Proton Scattering @ HERA

Scattered
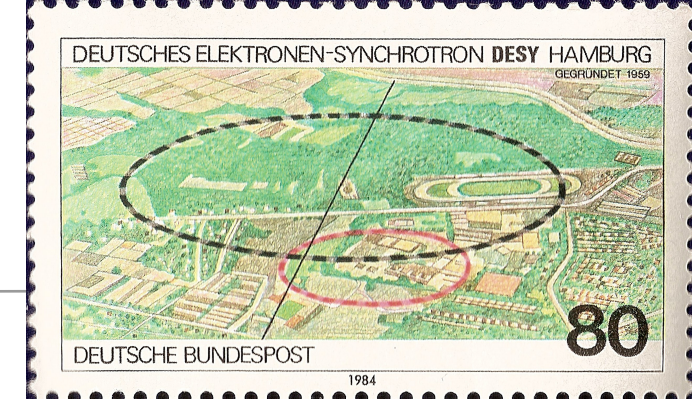## Electron

Electron-Proton
Scattering

Electron

Proton

Scattered
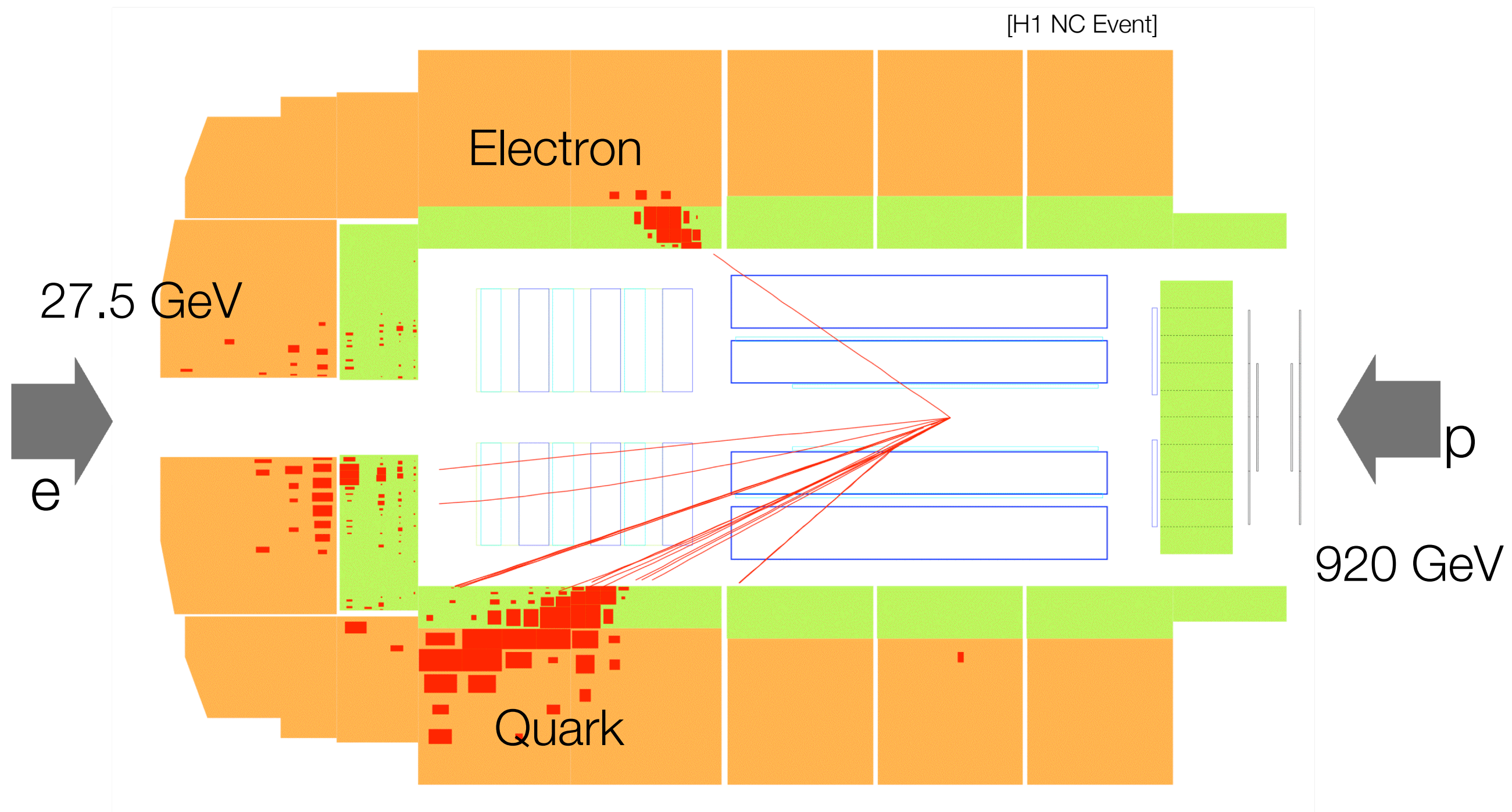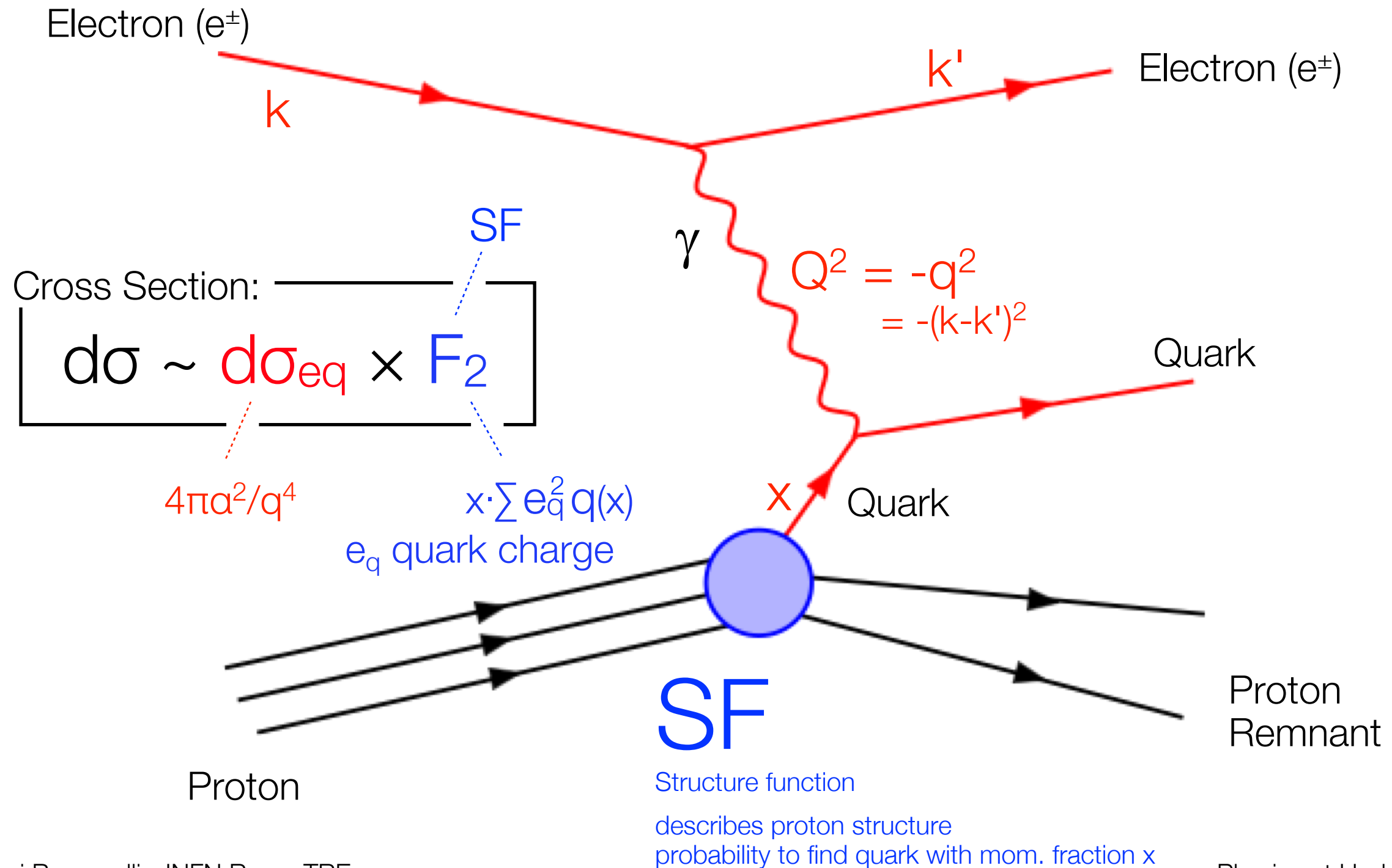## Quark
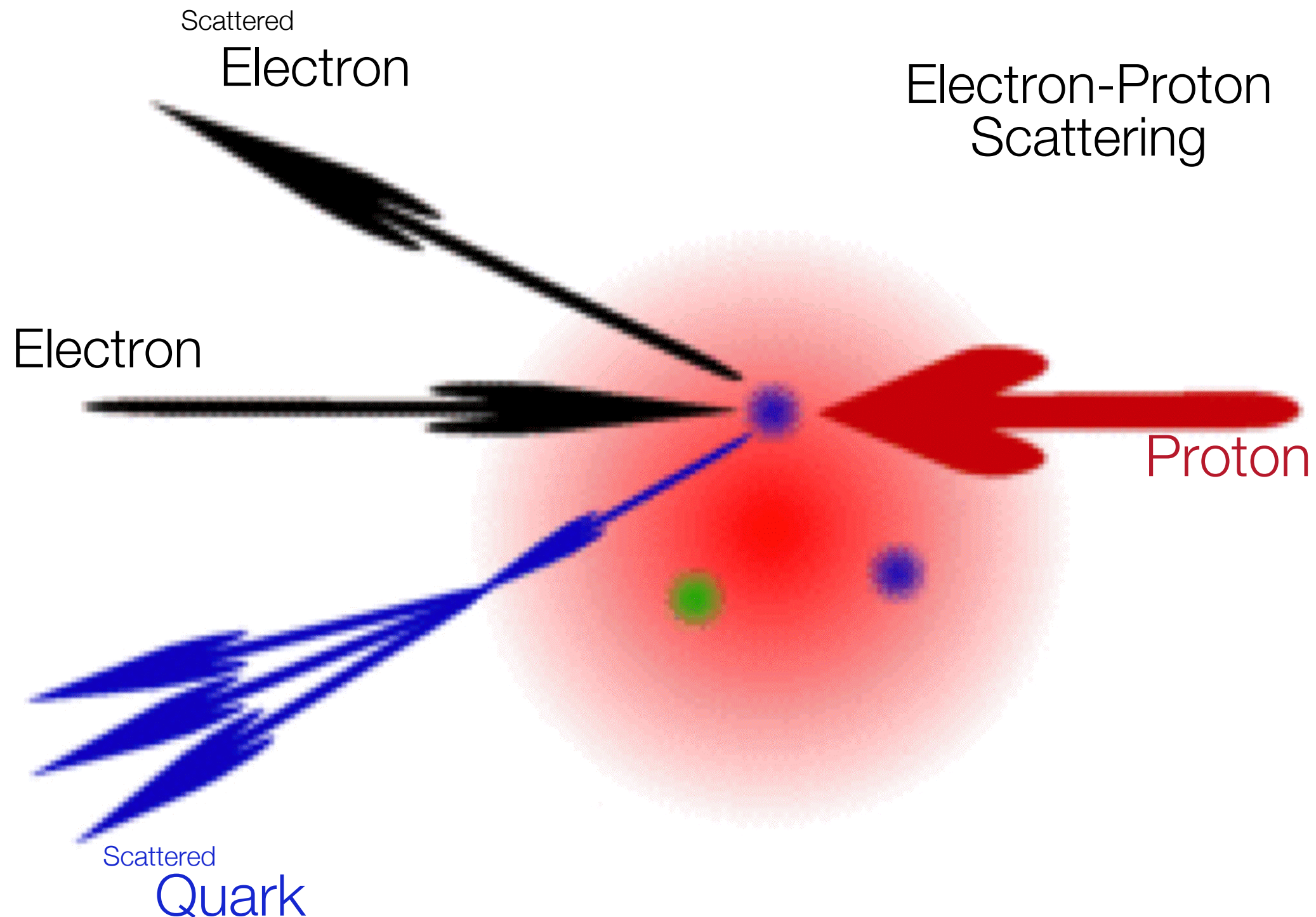
Hera Accelerator at Desy
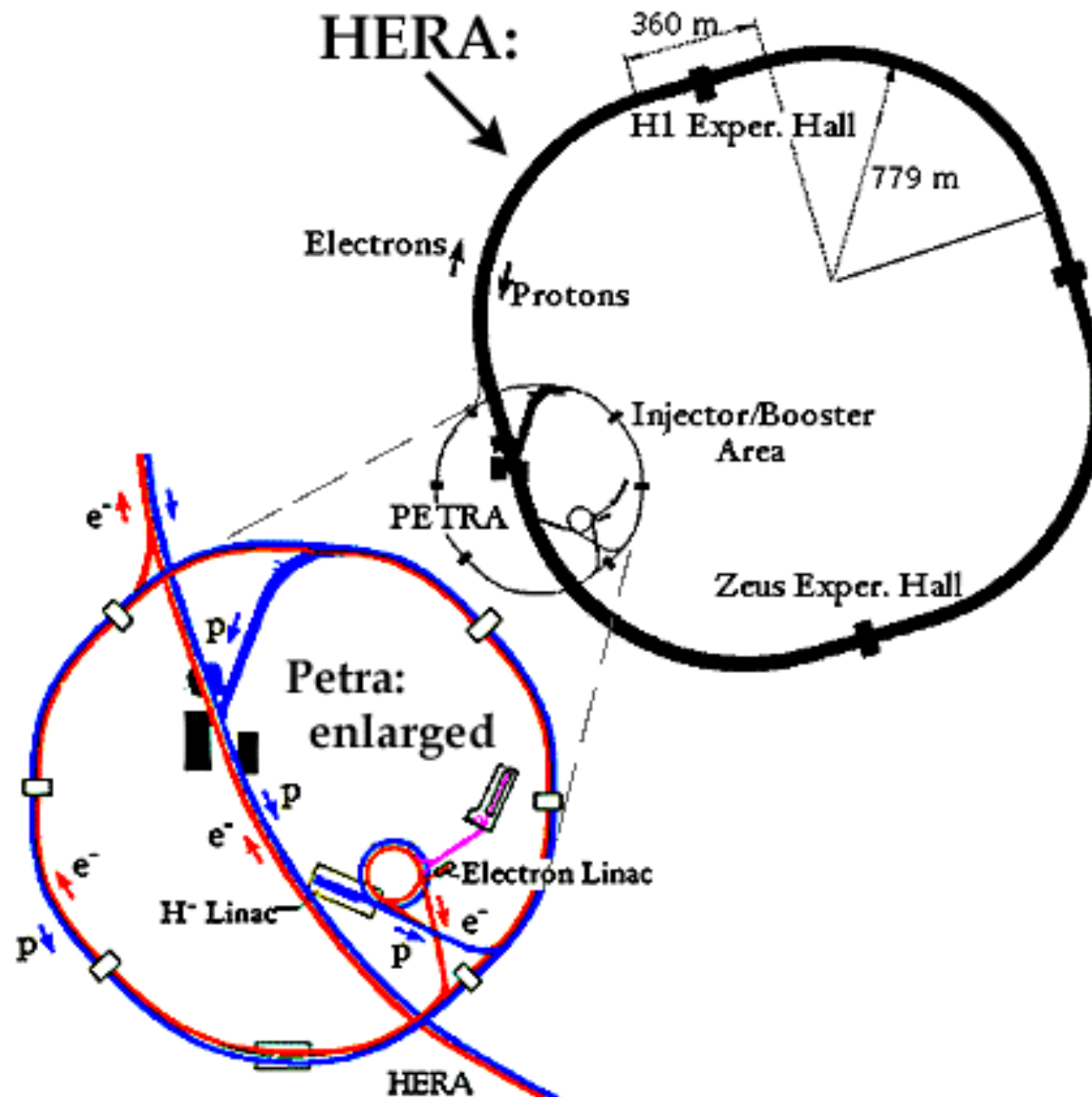
HERA

HERA was an Hadron-Electron Ring Accelerator in Desy, Hamburg-DE. It began operating in 1992 around 15 to 30 m underground and has a circumference of 6.3 km. . At HERA, electrons or positrons were collided with protons at a cms energy of 318 GeV. HERA was closed down on 30 June 2007. The HERA tunnel is located under the DESY site and the nearby Volkspark Leptons and protons were stored in two independent storage rings on top of each other inside this tunnel. There are four interaction regions, which were used by the experiments H1, ZEUS, HERMES and Hera-B. Leptons (electrons or positrons) were pre-accelerated to 450 MeV in the linear accelerator *LINAC-II*. From there they were injected into the storage ring *DESY-II* and accelerated further to 7.5 GeV before their transfer into *PETRA*, where they were accelerated to 14 GeV. Finally they were injected into their storage ring in the HERA tunnel and reached a final energy of 27.5 GeV. This storage ring was equipped with warm (non-superconducting) magnets keeping the leptons on their circular track by a magnetic field of 0.17 Tesla. Protons were obtained from originally negatively charged hydrogen ions and pre-accelerated to 50 MeV in a linear accelerator. They were then injected into the proton synchrotron *DESY-III* and accelerated further to 7 GeV. Then they were transferred to PETRA where they were accelerated to 40 GeV. Finally, they were injected into their storage ring in the HERA tunnel and reached their final energy of 920 GeV. The proton storage ring used superconducting magnets to keep the protons on track. The characteristic build-up time expected for the HERA accelerator was approximately 40 minutes.

Electron-Proton Scattering @ HERA

[H1 NC Event]

Electron

27.5 GeV

e

p

920 GeV

Quark

Electron-Proton Scattering @ HERA

Electron (e$^\pm$)

k

k'

Electron (e$^\pm$)

SF

Cross Section:

$$d\sigma \sim d\sigma_{eq} \times F_2$$

γ

$Q^2 = -q^2$

$= -(k-k')^2$

Quark

$4\pi\alpha^2/q^4$

$x \cdot \sum e_q^2 q(x)$

e_q quark charge

x Quark

Proton Remnant

SF

Proton

Structure function

describes proton structure
probability to find quark with mom. fraction x

Structure Function F$_2$

e — e

Electron-Quark scattering

(spinless case)

q

q
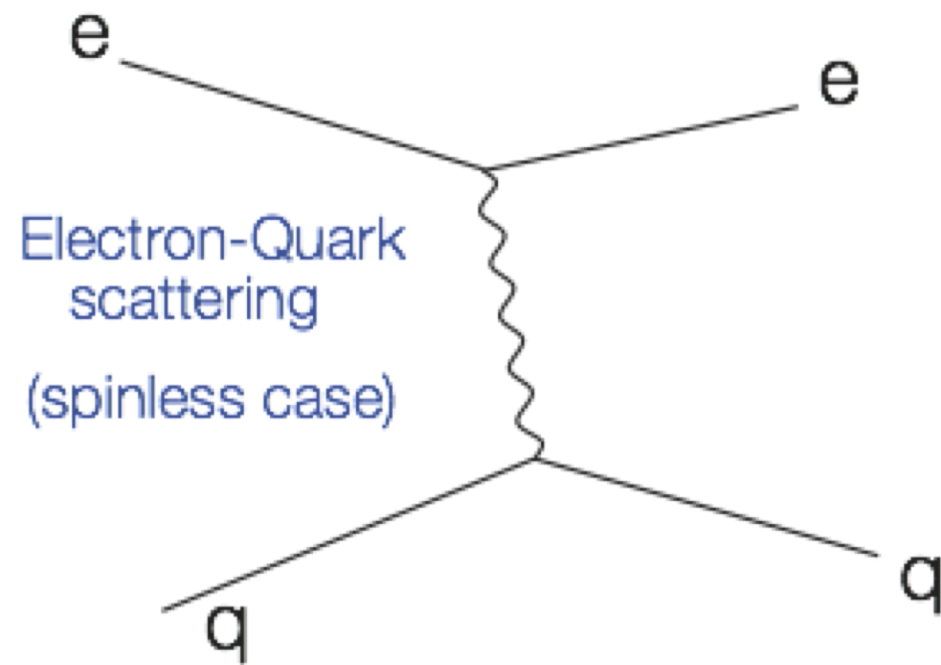
Naive **QPM**

$$\frac{d\sigma(eq)}{dq^2} = \frac{4\pi\alpha^2}{q^4}e_q^2$$

Rutherford scattering on pointlike target

$xq(x)$

$p = |uud\rangle$
$x = 1/3$

1/3   x

$$\frac{d\sigma(ep)}{dq^2} = \frac{4\pi\alpha^2}{q^4}[2e_u^2 + e_d^2] = \frac{4\pi\alpha^2}{q^4}$$
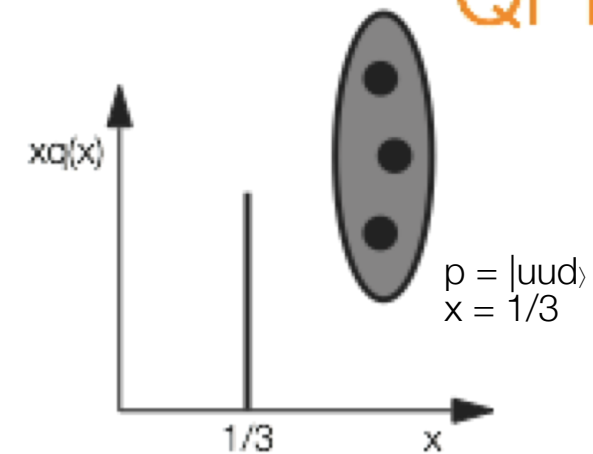
With quark-quark interactions

$xq(x)$
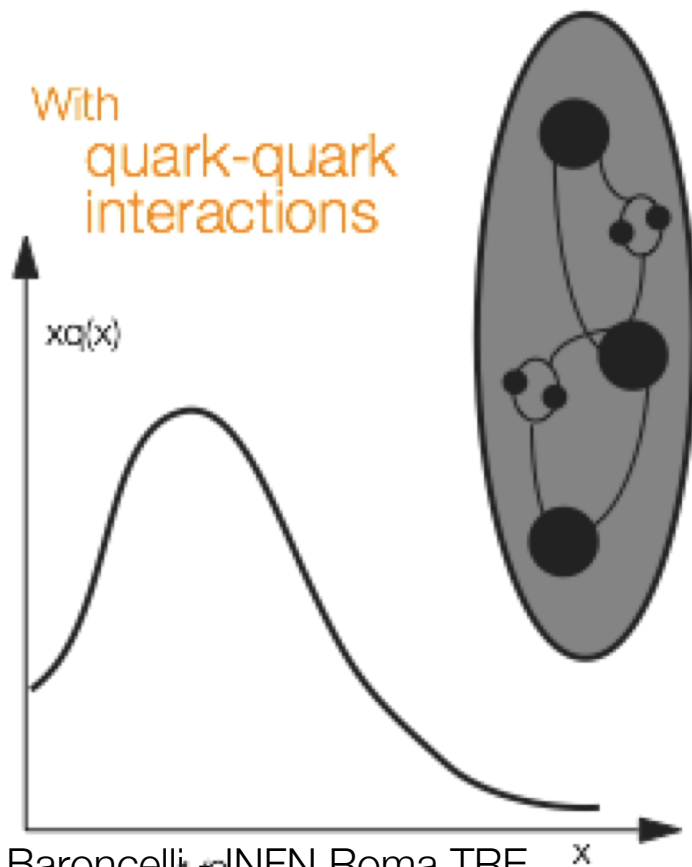
$$\frac{d\sigma(ep)}{dx\,dq^2} = \frac{4\pi\alpha^2}{q^4}[e_u^2 u(x) + e_d^2 d(x) + \ldots]$$

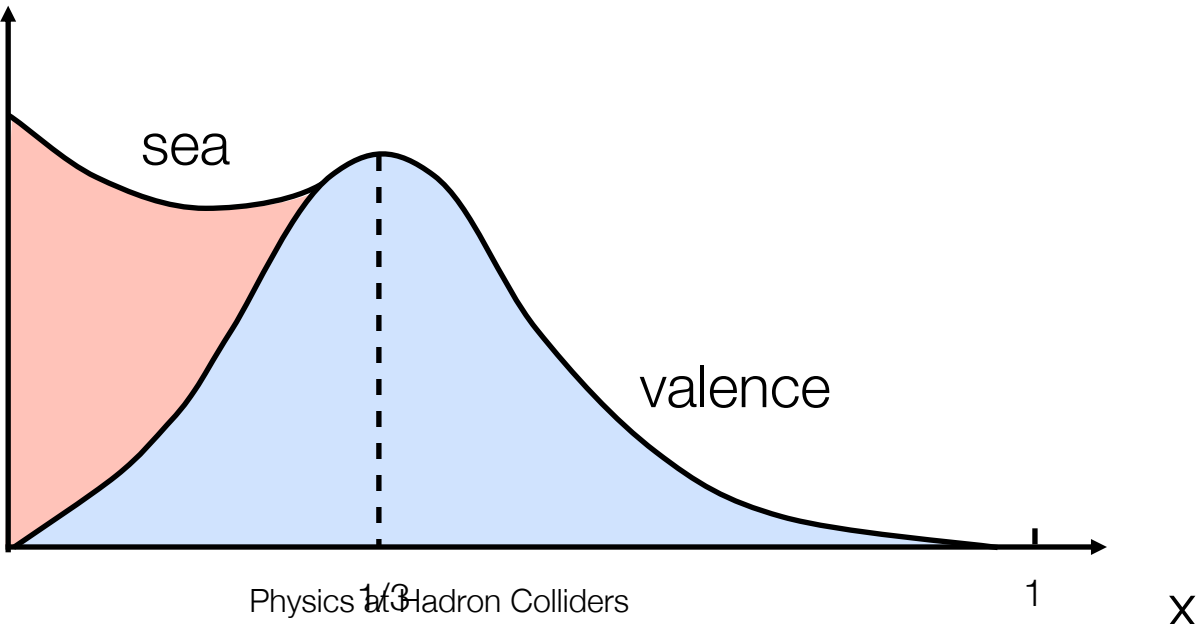$$= \frac{4\pi\alpha^2}{q^4}\frac{F_2(x)}{x}$$

QPM: Structure Functions F$_2$ independent of Q^2

F₂(x)

Proton — Three valence quarks

Proton — Three bound valence quarks

Proton — Bound valence quarks + gluon radiation

[see e.g. Halzen/Martin]

small x

1/3

1

x

1/3

1

x

sea

valence

1/3

1
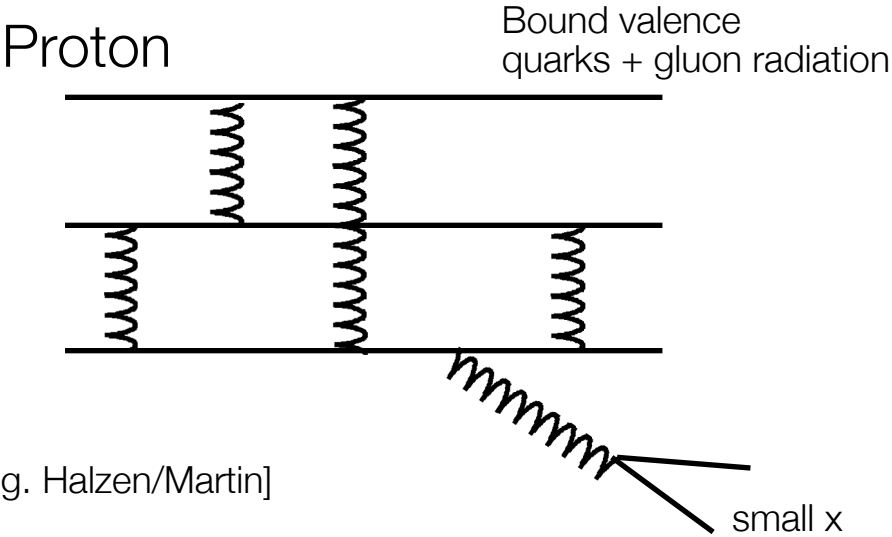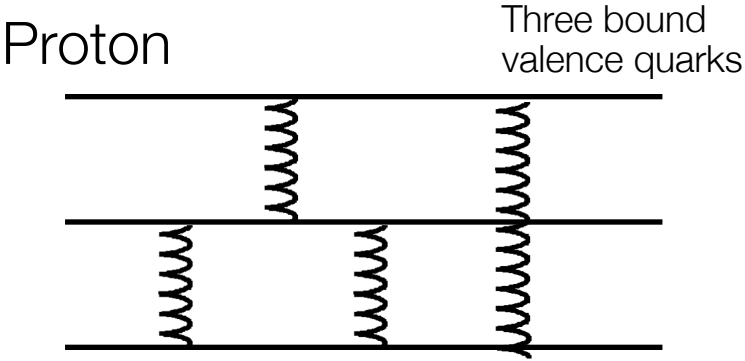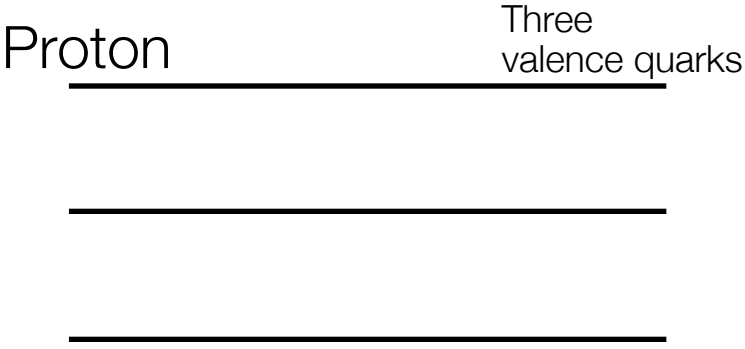
x
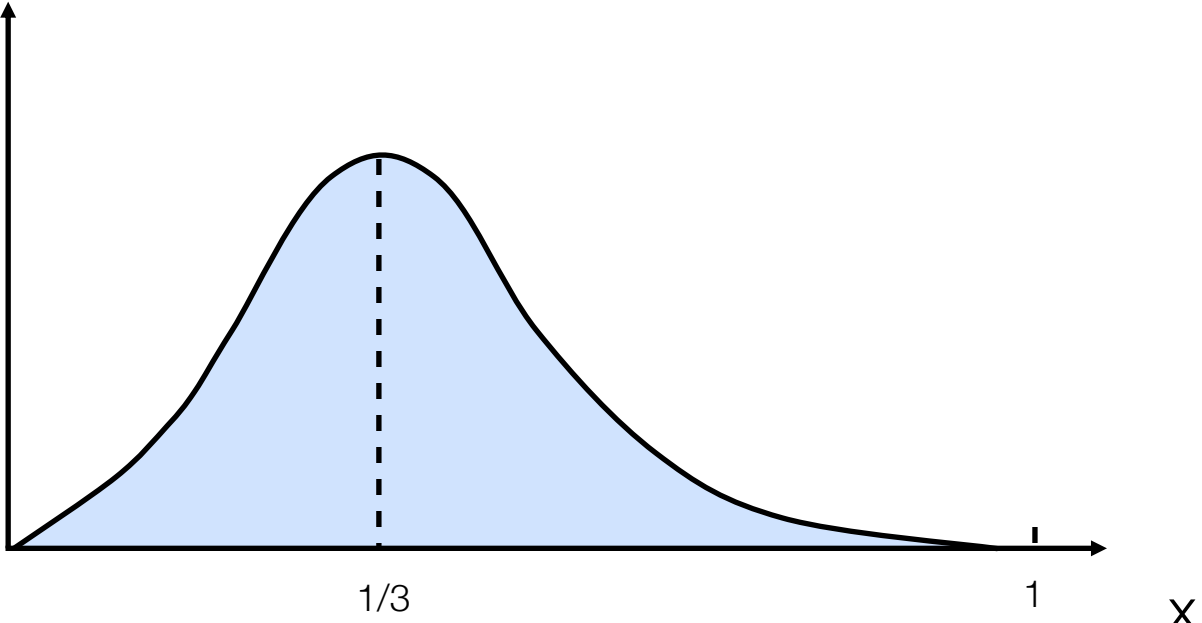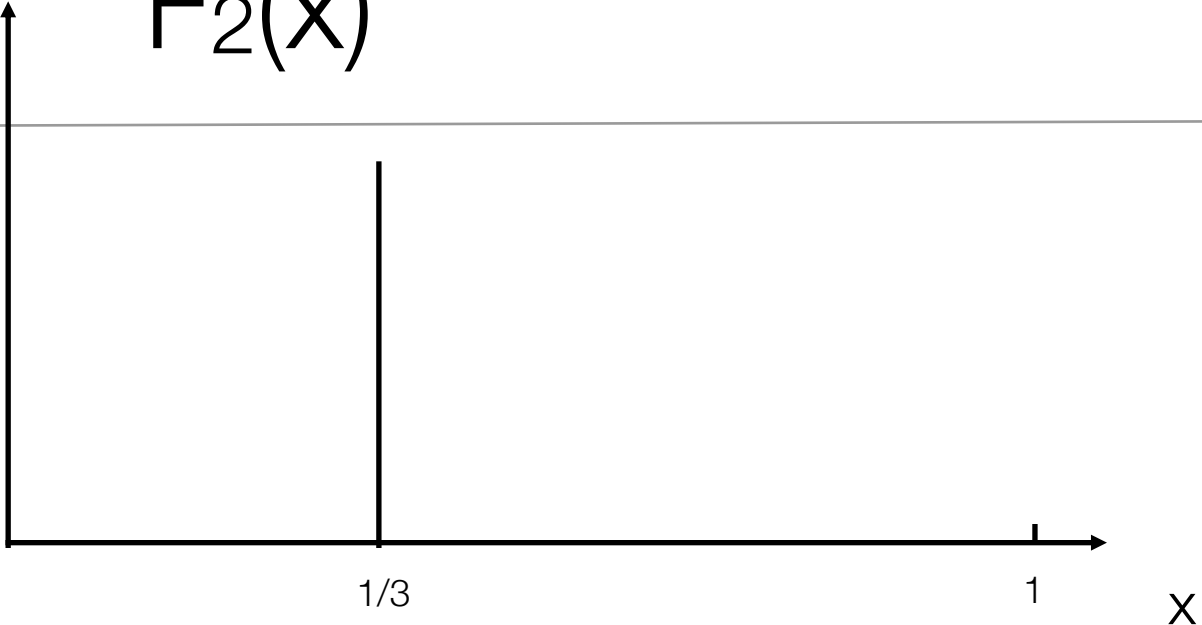
Invariant Quantities in DIS
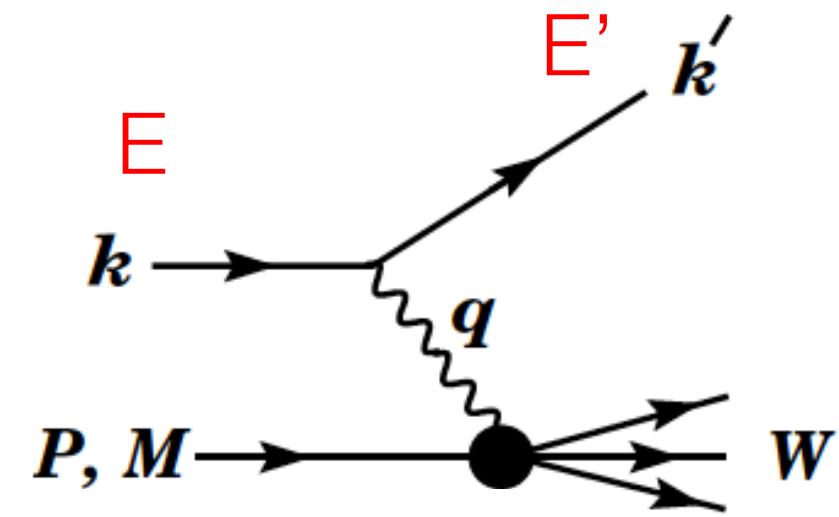
Invariant quantities:

$$\nu = \frac{q \cdot P}{M} = E - E'$$ is the lepton's energy loss in the nucleon rest frame (in earlier literature sometimes $\nu = q \cdot P$). Here, E and E' are the initial and final lepton energies in the nucleon rest frame.

$$Q^2 = -q^2 = 2(EE' - \vec{k} \cdot \vec{k}') - m_\ell^2 - m_{\ell'}^2$$ where $m_\ell (m_{\ell'})$ is the initial (final) lepton mass. If $EE' \sin^2(\theta/2) \gg m_\ell^2, m_{\ell'}^2$, then

$$\approx 4EE' \sin^2(\theta/2),$$ where θ is the lepton's scattering angle with respect to the lepton beam direction.

$$x = \frac{Q^2}{2M\nu}$$ where, in the parton model, x is the fraction of the nucleon's momentum carried by the struck quark.

$$y = \frac{q \cdot P}{k \cdot P} = \frac{\nu}{E}$$ is the fraction of the lepton's energy lost in the nucleon rest frame.

$$W^2 = (P + q)^2 = M^2 + 2M\nu - Q^2$$ is the mass squared of the system X recoiling against the scattered lepton.

$$s = (k + P)^2 = \frac{Q^2}{xy} + M^2 + m_\ell^2$$ is the center-of-mass energy squared of the lepton-nucleon system.

8. Deep inelastic scattering.

In lepton-hadron scattering at sufficiently high energies one finds a large number of hadrons in the final state: this is *deep inelastic scattering* (DIS). The multiplicity of the hadronic system varies event by event. The reaction equation for electron-proton DIS is written as

$$e^- + p \rightarrow e^- + X \tag{84}$$

where X stands for the hadronic system with an arbitrary number of particles. A generic diagram depicting the DIS process is shown in Fig. 2.
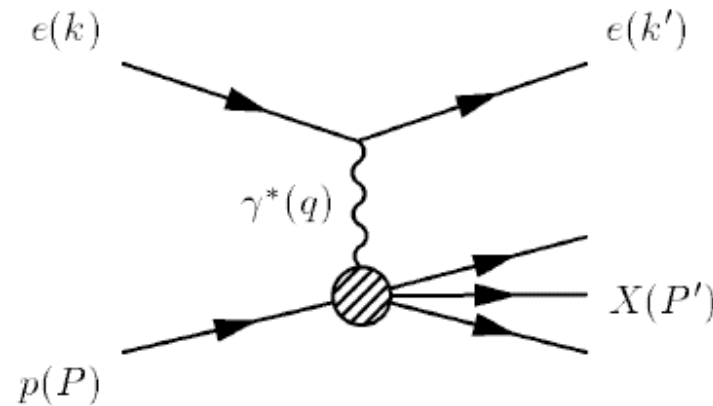
Figure 2: Generic diagram of deep inelastic scattering.

To describe the DIS reaction kinematics we denote the 4-momentum of the incoming electron by $k = (E, 0, 0, k)$, that of the target proton by P and those of the scattered electron and of the hadronic system by k' and P', respectively. The exchanged virtual photon γ^* has 4-momentum $q = k - k'$. 4-momentum conservation demands

$$k + P = k' + P' \tag{85}$$

and we have the mass-shell conditions $k^2 = k'^2 = m_e^2$ and $P^2 = m_p^2$. Since energies characteristic of DIS are at least of several GeV, the electron mass can be safely set equal to zero. Then we get for the square of the 4-momentum transfer $q^2 = (k - k')^2 = -2EE'(1 - \cos\theta)$, and we see that $q^2 \leq 0$, *i.e.* the exchanged photon is space-like.

The invariant $W^2 = P'^2$ is variable because of the variable multiplicity of particles in the hadronic system, each of which can have an arbitrary kinetic energy up to some maximum value. Therefore the complete kinematics of DIS is determined by three independent invariants rather than two as we are used to in elastic collisions. A natural choice of one of these invariants is the square of the total CMS energy S,

$$S = (k + P)^2 = m_p^2 + 2k \cdot P \tag{86}$$

which is defined by the beam energy.

The second invariant is usually chosen to be the negative square of 4-momentum transfer:

$$Q^2 = -q^2 = -(k - k')^2 = 4EE' \sin^2 \frac{\theta}{2} \tag{87}$$

The third independent invariant can be taken to be W or alternatively one of the dimensionless variables

$$x = \frac{Q^2}{2P \cdot q} \tag{88}$$

or

$$y = \frac{P \cdot q}{k \cdot P} \tag{89}$$

where $q = k - k'$.

The variable y has a simple physical meaning in the target rest frame where $P = (m_p, 0, 0, 0)$, $k = (E_{\text{LAB}}, 0, 0, E_{\text{LAB}})$, and $k' = (E'_{\text{LAB}}, \vec{p_3})$, hence $y = 1 - E'_{\text{LAB}}/E_{\text{LAB}}$, i.e. y is the relative energy loss of the electron in the LAB frame.

The invariant x is the Bjorken scaling variable or simply Bjorken-x. It was first recognised as an important variable of DIS by J.D. Bjorken who predicted the property of scaling in DIS which was subsequently confirmed experimentally.

Interesting is the expression of S in terms of the beam energies. In fixed target DIS we have the electron or muon beam with 4-momentum $k = (E, 0, 0, E)$ and the proton target with $P = (m_p, 0, 0, 0)$, hence

$$S = m_p^2 + 2m_p E$$

whereas in an electron-proton collider like HERA we have 4-momenta $P = (E_p, 0, 0, E_p)$ and $k = (E_e, 0, 0, -E_e)$ and hence

$$S = 4E_e E_p$$

Other useful relations between the various kinematical variables are the following:

$$Q^2 = xyS \tag{90}$$

and

$$W^2 = m_p^2 + Q^2(1/x - 1) \tag{91}$$

where in the latter formula we have kept the proton mass in order to indicate that the threshold of W corresponds to elastic scattering.

Within the framework of the parton model, DIS proceeds by the exchange of a photon or intermediate vector boson with only one of the quarks in the proton. This is shown in the diagram in Fig. 3.

The electron-quark collision is elastic. As a result of this collision the struck quark acquires a sufficient momentum to break away from the rest of the proton as far as the colour force allows it to travel. At this stage some of the binding energy is converted into the creation of a quark-antiquark pair from the vacuum; the antiquark combines with the original quark into a meson, leaving behind a quark which can give rise to the creation of another quark-antiquark
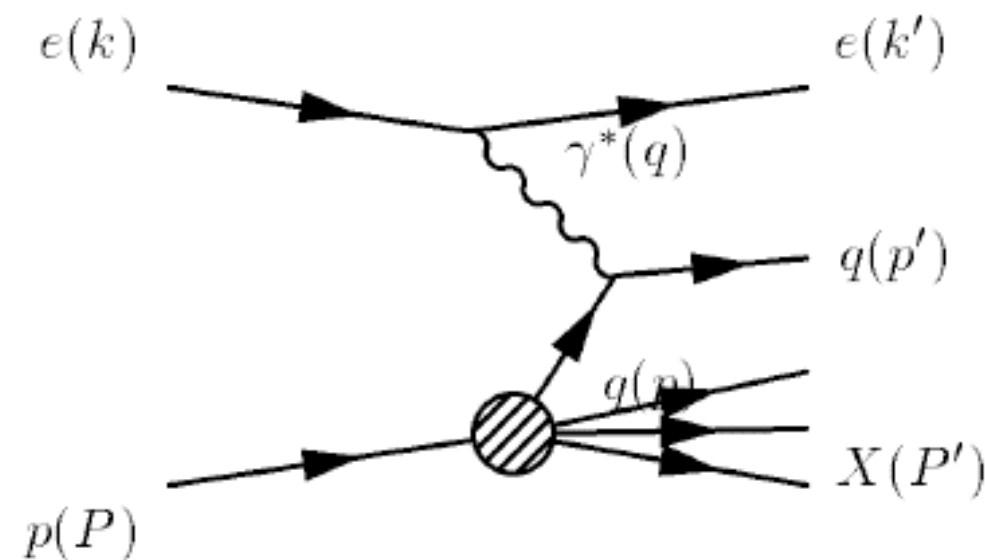

Figure 3: Parton model diagram of deep inelastic scattering.

pair. This process, called *fragmentation*, continues until the remaining energy drops below the threshold for the creation of another pair. Thus, as a result of fragmentation, several mesons are created which travel roughly in the direction of the struck quark. Such a system of mesons, or more generally of hadrons, is called a *jet*. The residue of the proton is a highly unstable system: it has lost a quark, absorbed a quark presumably of the wrong sort that is left over from the fragmentation, and has absorbed a fraction of the energy transferred from the electron. Therefore it breaks up into several hadrons.

The elastic electron-quark collision is the *hard subprocess* of DIS. If we think of the incoming electron and proton as travelling in opposite directions, then the quark carries a fraction of the proton momentum. At a sufficiently high momentum, where the proton mass is negligible, the energy of the quark is the same fraction of the proton energy. It turns out that this fraction is identical with the Bjorken-x defined above. Denoting the 4-momentum of the incoming quark by p we have therefore

$$p = xP$$

Denoting the invariant $(k+p)^2$ by s, which is the squared CMS energy of the subprocess, we have therefore also

$$s = xS \tag{92}$$

This, together with the definition of Q^2, shows that the two independent invariants that control the kinematics of the subprocess are x and Q^2.

The first DIS experiments were carried out in 1967 at the Stanford 2-mile linear electron accelerator with electron beams of up to 20 GeV and hydrogen targets at rest, giving a CMS energy of about 6 GeV. Subsequent fixed target experiments were done in other laboratories, notably at the CERN SPS with muon beams of up to nearly 300 GeV and hence of CMS energies up to about 25 GeV. The range of energies available for DIS was extended by an order of magnitude when in 1992 the electron-proton collider HERA came into operation at the DESY laboratory in Hamburg. In this collider the electrons are accelerated up to nearly 30 GeV and the protons up to 820 GeV, giving a CMS energy of 314 GeV. Theoretically the corresponding values of Q^2 go up to about 10^5 GeV^2.

An important tool to study the structure of the nucleon is also deep inelastic scattering with neutrinos as beam particles. The kinematics is identical with the one described above, but one must bare in mind that the exchanged particle in neutrino-DIS is an intermediate vector boson, either the W or the Z.

$$F_1(x, Q^2) \rightarrow \tfrac{1}{2} \sum_f Q_f^2 \big(q_f(x) + \overline{q}_f(x) \big) . \tag{28}$$

The result in Eq. (28) demonstrates that F_1 depends only on the dimensionless variable $x = Q^2/2\nu$ in the deep inelastic limit, which is known as Bjorken scaling[5, 6]. The experimental observation of this scaling was the first direct evidence for point-like constituents in hadrons[7]. The quark distribution functions $q_f(x)$, $\overline{q}_f(x)$ defined by Eq. (26) for $x \geq 0$ are an intrinsic non-perturbative property of the hadron H. They may be interpreted as momentum distributions for quarks and anti-quarks inside the hadron and in principle (thought not yet in practice) they can be computed from a non-perturbative analysis in QCD. At present these distribution functions must simply be determined experimentally from (largely) DIS experiments. We also find that

$$F_2(x, Q^2) = 2x F_1(x, Q^2) = x \sum_f Q_f^2 \big(q_f(x) + \overline{q}_f(x) \big) . \tag{29}$$

The form of the relation between F_1 and F_2 is a consequence of the spin $1/2$ nature of the struck quark. The difference is proportional to the longitudinal structure function $F_L(x, Q^2)$, and is zero at lowest order due to helicity conservation[8].

Applying these results to deep inelastic scattering on a proton target the proton wavefunction is dominated by $uud + \cdots$ where the dots indicate uud plus further quarks (including heavy flavours). With notation $q_u(x) = u(x)$, $\overline{q}_u(x) = \overline{u}(x)$ etc,
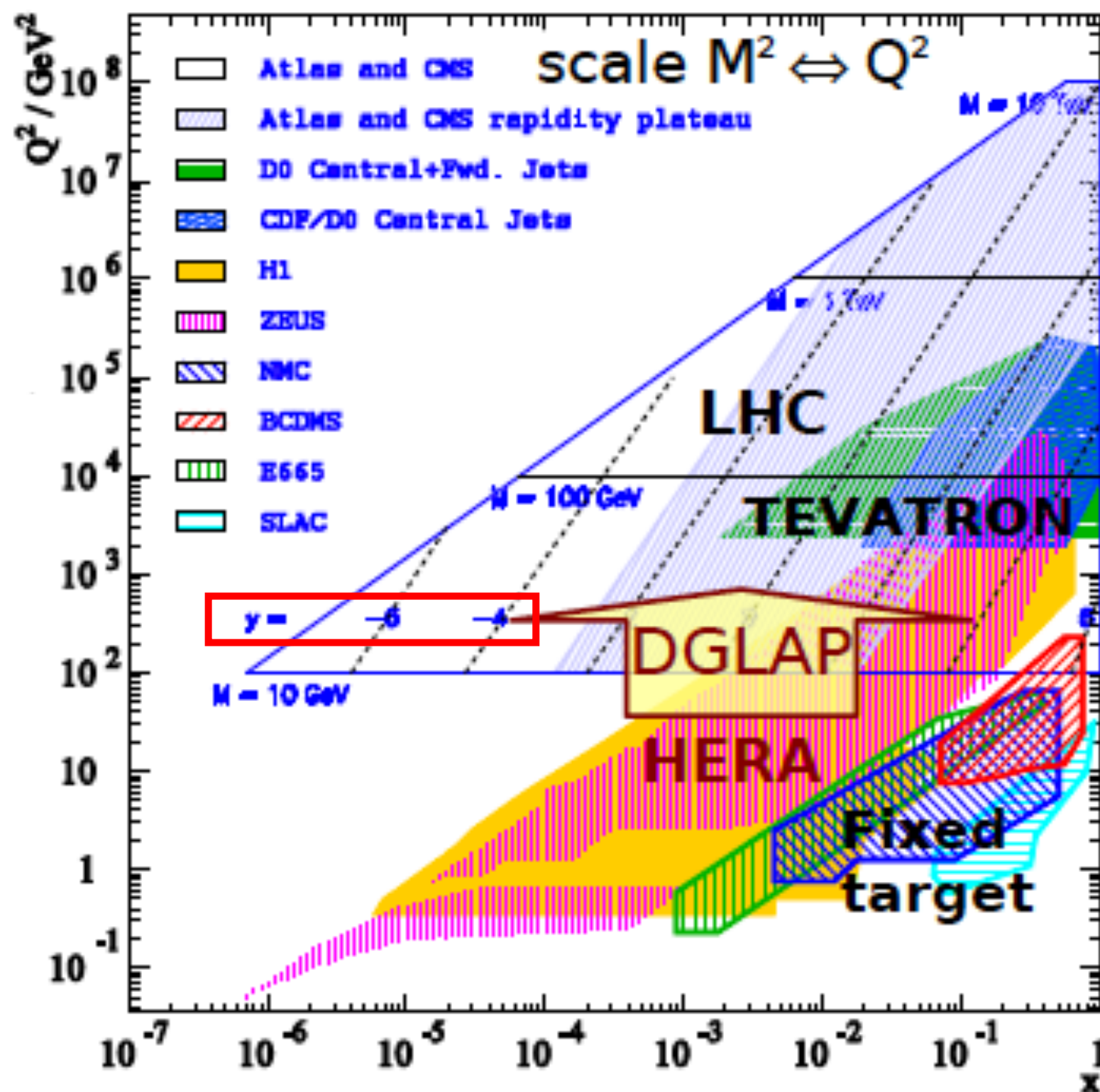
$$F_{2,\text{proton}}(x, Q^2) \sim x \Big(\tfrac{4}{9}(u(x) + \overline{u}(x)) + \tfrac{1}{9}(d(x) + \overline{d}(x)) + \text{ heavy flavours} \Big) . \tag{30}$$

We note that the derivation of Eq. (28) is an approximation which relies on the assumption that k, being the the momentum of a quark (or antiquark) inside the proton, should have a very small probability of having any momentum components greater than $\mathcal{O}(\Lambda_{QCD})$. As such it also implies corrections of $\mathcal{O}(\Lambda_{QCD}^2/Q^2)$ corresponding to higher twist operators (as discussed in[9]). However, it also ignores
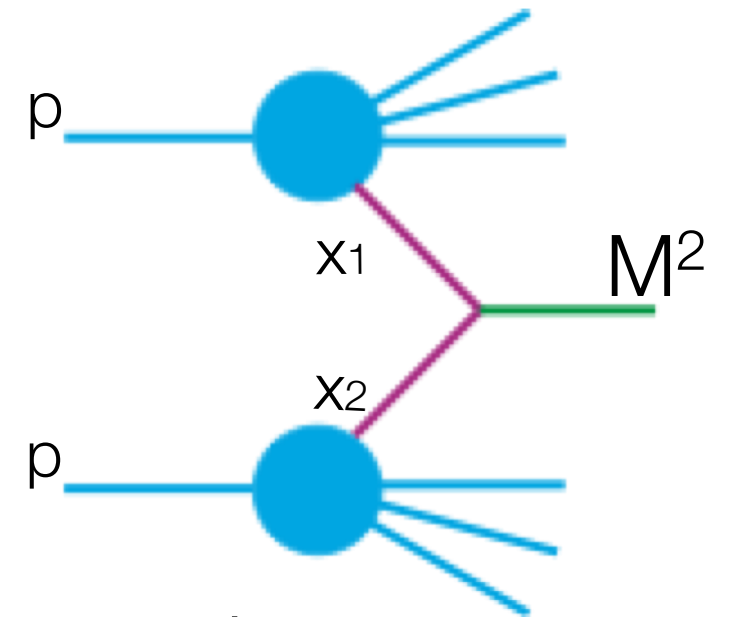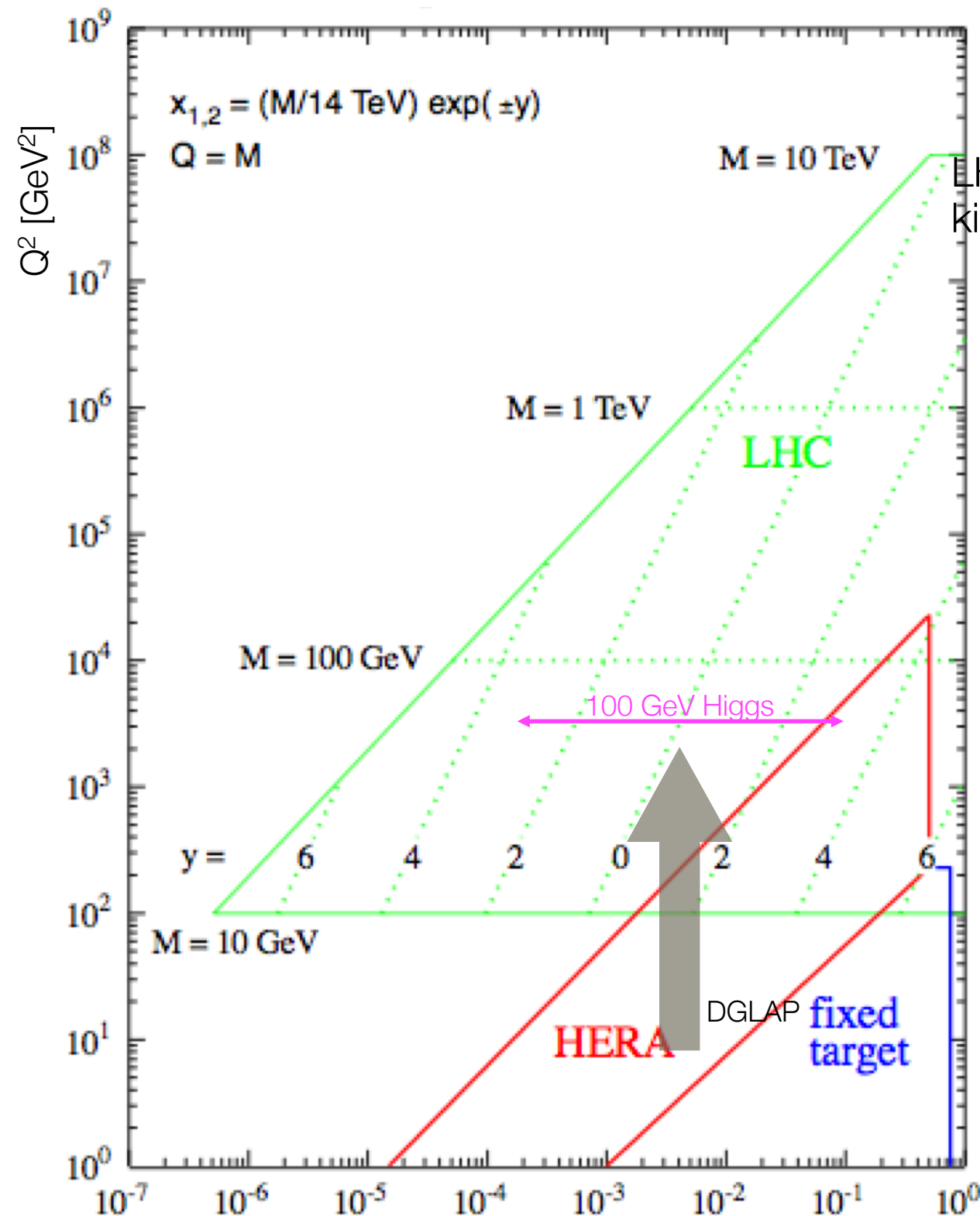
mass of the recoiling quark against the lepton

$$W^2 = m_p^2 + Q^2(1/x - 1)$$

Particle Production @ LHC

LHC parton kinematics

$x_{1,2} = (M/14 \text{ TeV}) \exp(\pm y)$

$Q = M$

$M = 10$ TeV

$M = 1$ TeV

LHC

$M = 100$ GeV

100 GeV Higgs

$M = 10$ GeV

$y = $ 6 4 2 0 2 4 6

HERA

DGLAP fixed target

Q^2 [GeV^2]

x

pp ➤ X$_M$ + remnants

X$_M$: particle with mass M
e.g. Higgs

$M^2 = x_1 x_2 \cdot s$

i.e. to produce a particle with mass M at LHC energies ($\sqrt{s} = 14$ TeV)
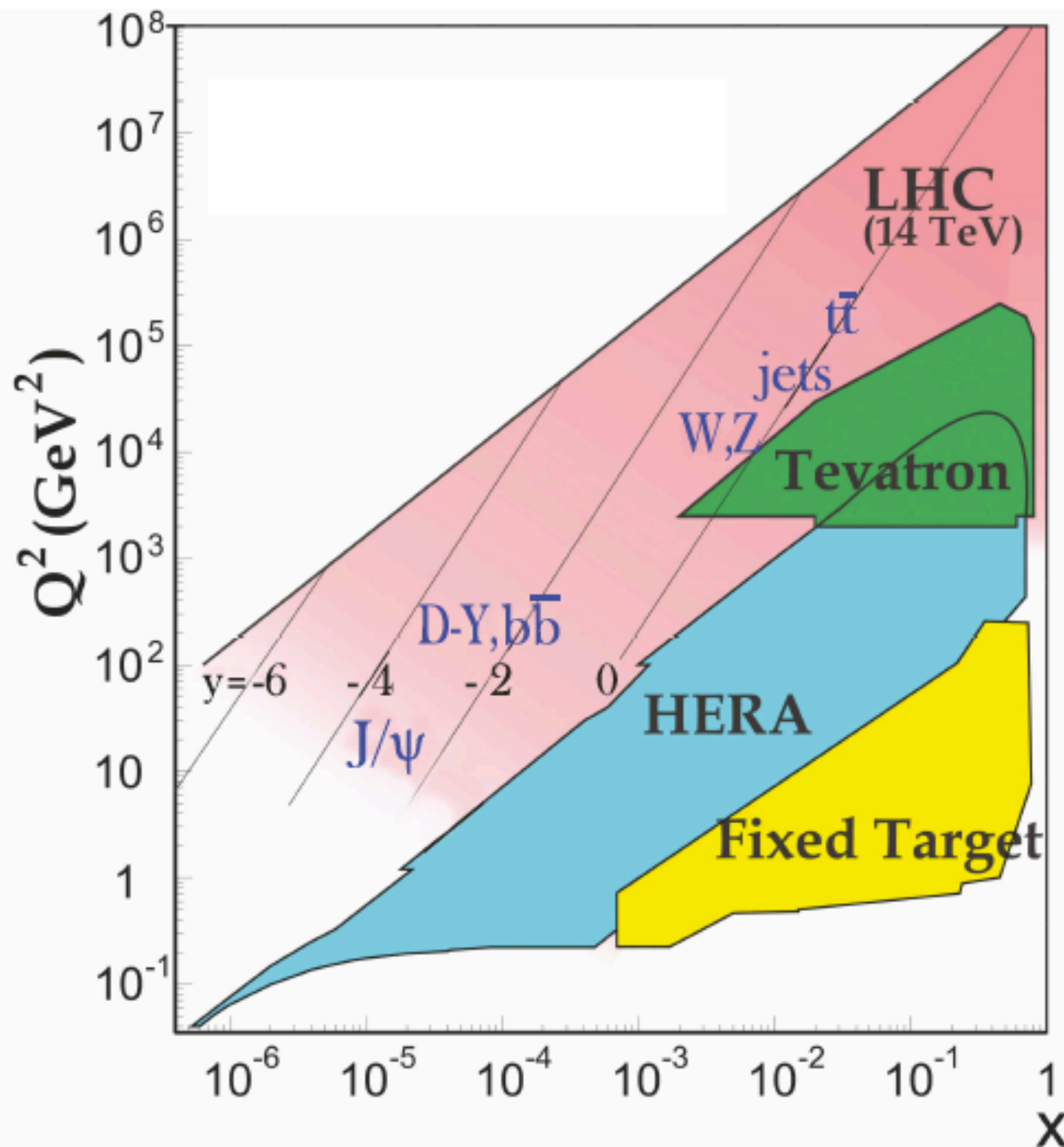
$\langle x \rangle = \sqrt{x_1 x_2} = M/\sqrt{s}$

[$x_1 = x_2$: mid-rapidity]

p

p

x_1

x_2

M^2

LHC needs:

Knowledge of parton densities
Extrapolation over orders of magnitudes

Kinematic domains in DIS

Kinematic domains in x and Q^2 probed by fixed-target and collider experiments. Some of the final states accessible at the LHC are indicated in the appropriate regions, where y is the rapidity. The incoming partons have

$$x_{1,2} = (M/14\ \text{TeV})e^{\pm y}$$

with Q = M where M is the mass of the state shown in blue in the figure. For example, exclusive J/ψ and upsilon production at high |y| at the LHC may probe the gluon PDF down to x ∼ 10–5.

Physics at Hadron Colliders

[z: momentum fraction of radiated parton]

[DGLAP: Dokshitzer, Gribov, Lipatov, Altarelli, Parisi]

$$\frac{4}{3}\left[\frac{1+z^2}{1-z}\right]$$

$$\frac{1}{2}\left[z^2+(1-z^2)\right]$$

PDFs

$$\frac{\partial}{\partial \log Q^2}\begin{bmatrix} q(x,Q^2) \\ g(x,Q^2) \end{bmatrix} = \frac{\alpha_s}{2\pi}\begin{bmatrix} P_{q/q}\left[\ \right] & P_{q/g}\left[\ \right] \\ P_{g/q}\left[\ \right] & P_{g/g}\left[\ \right] \end{bmatrix} \otimes \begin{bmatrix} q(x,Q^2) \\ g(x,Q^2) \end{bmatrix}$$

$$\frac{4}{3}\left[\frac{1+(1-z)^2}{z}\right]$$

$$P\otimes f(x,Q^2)=\int_x^1 \frac{dy}{y}P(x/y)f(y,Q^2)$$

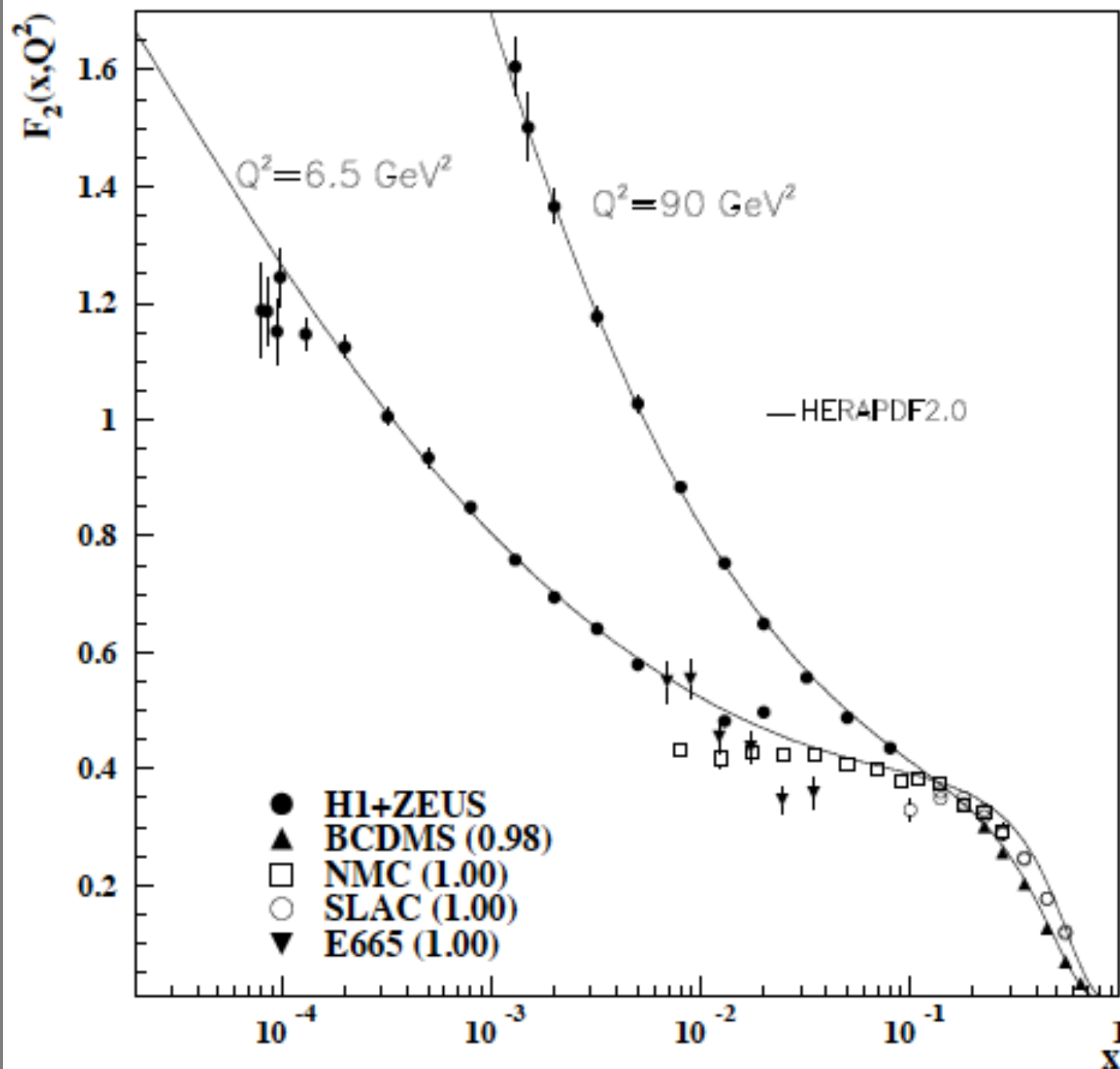$$6\left[\frac{z}{1-z}+\frac{1-z}{z}+z(1-z)\right]$$

Scaling violations in DIS

Increasing Q2 probes inner structure of proton
High x: naive parton model ⟹ Low x:finding gluons
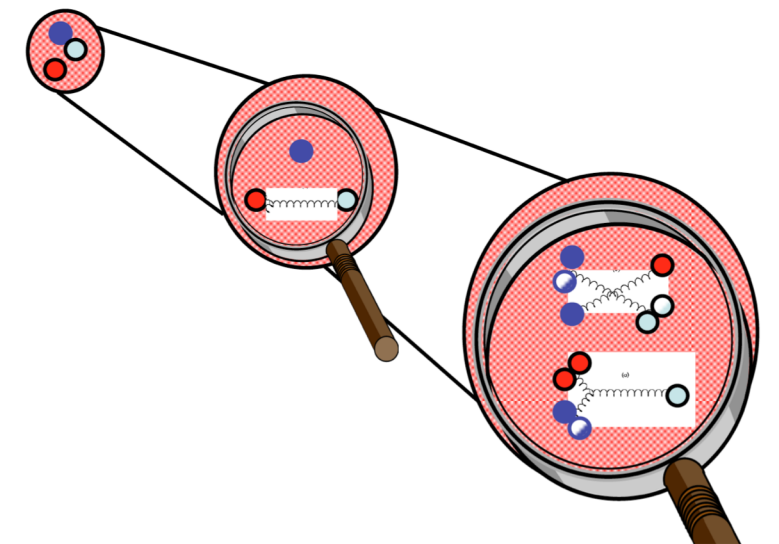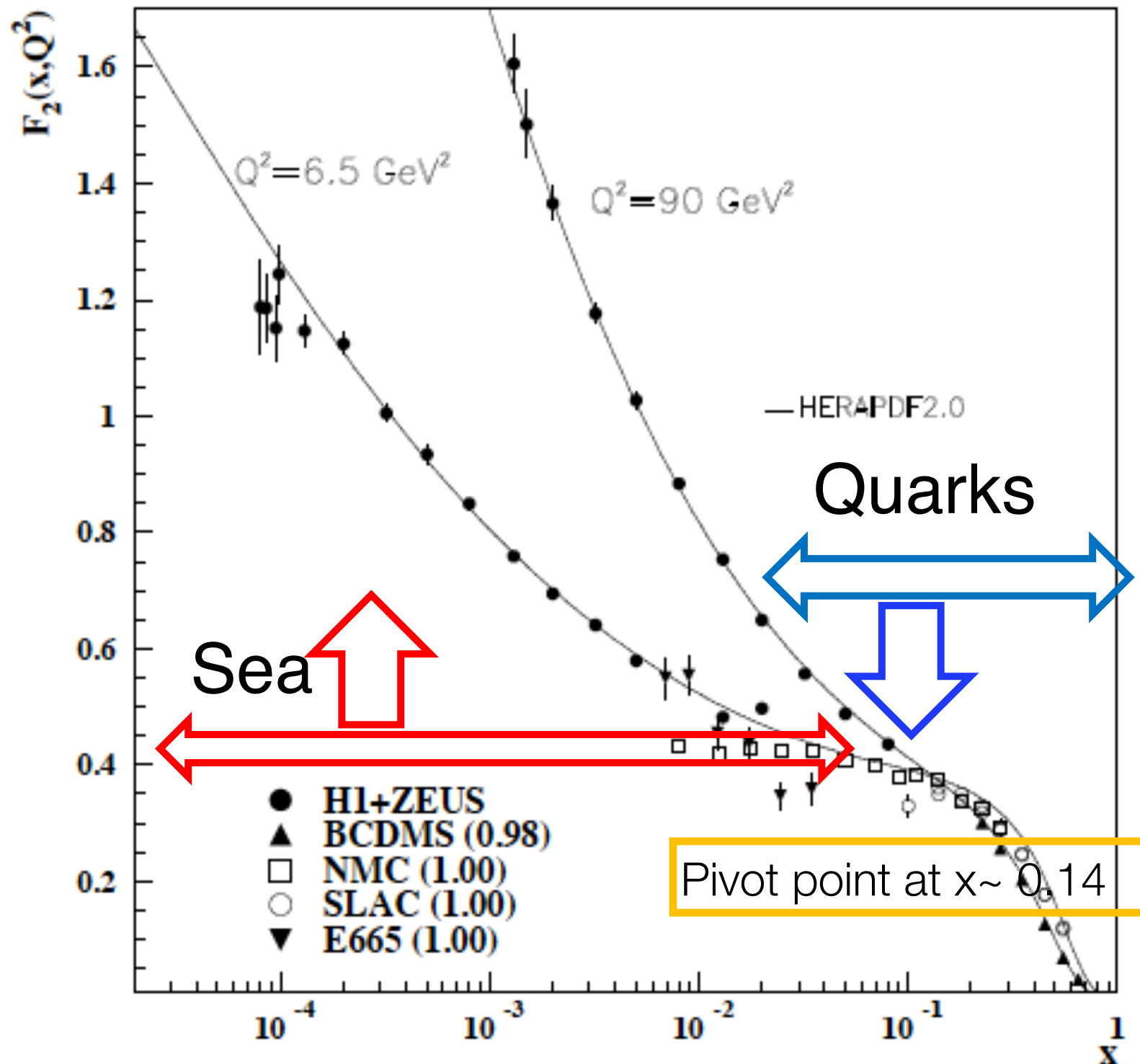

At low x we have gluon at high x we have quarks
Quarks: when Q^2 increases F2(x) goes down
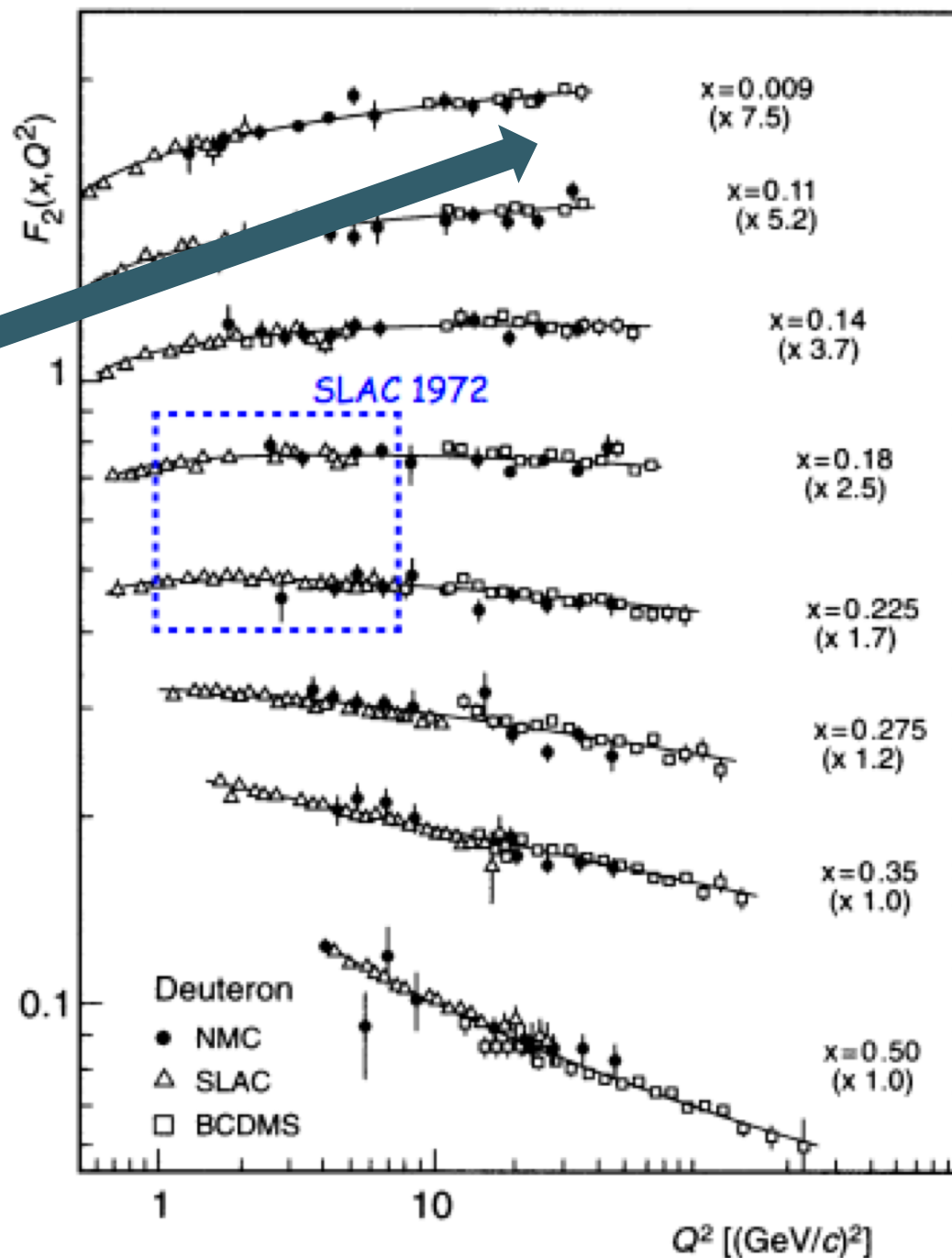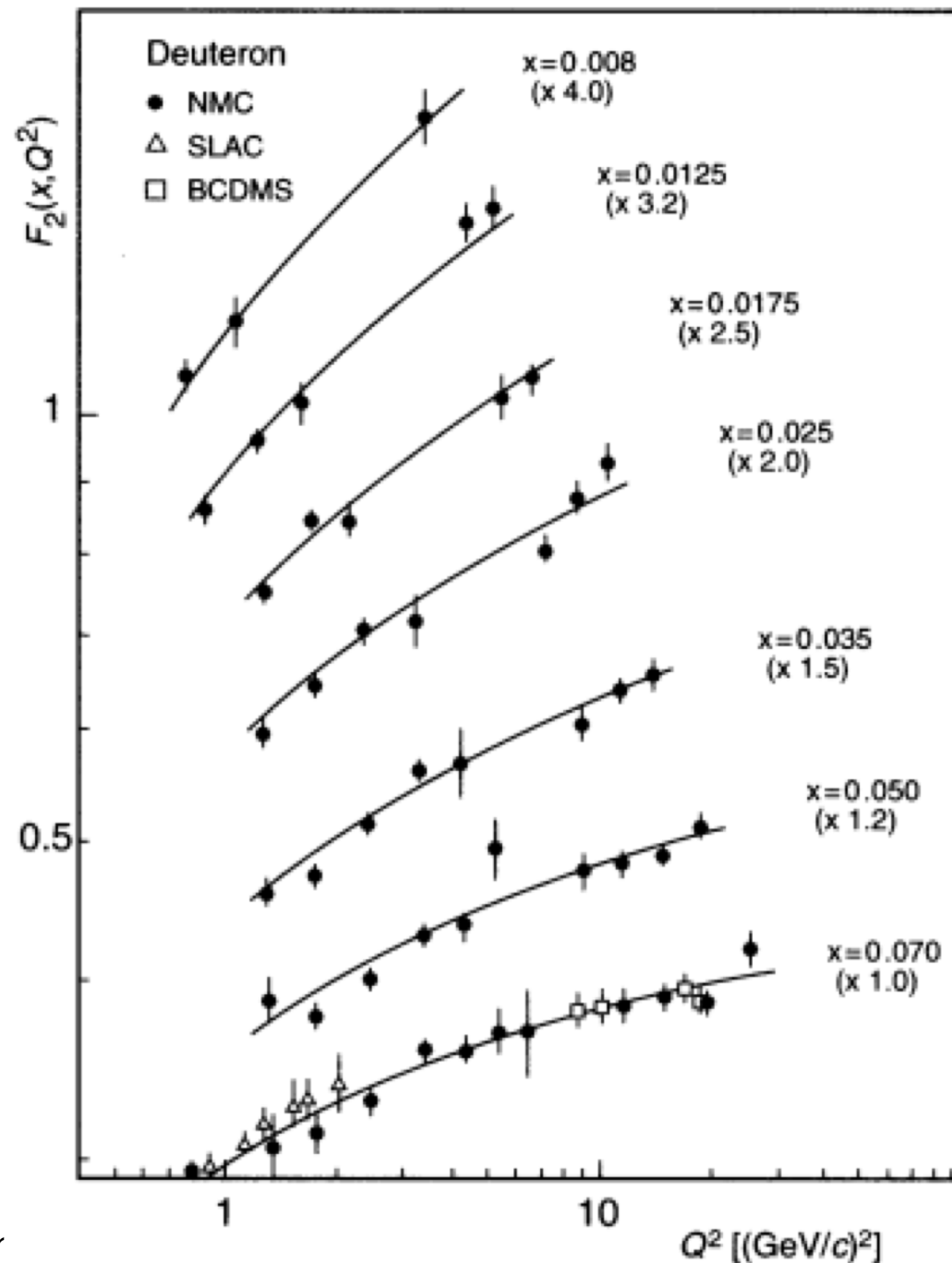Gluons: when Q2 increases F2(x) Goes up

Quarks

Sea

Pivot point at x~ 0.14

F2(x,Q²)

Q²=6.5 GeV²   Q²=90 GeV²

— HERAPDF2.0

• H1+ZEUS
▲ BCDMS (0.98)
□ NMC (1.00)
○ SLAC (1.00)
▼ E665 (1.00)

The proton structure function F^2 are given at two Q^2 values (6.5 GeV^2 and 90 GeV^2), which exhibit scaling at the 'pivot' point x ~ 0.14. The various data sets have been renormalized by the factors shown in brackets in the key to the plot, which were globally determined in a previous HERAPDF analysis [13]. The curves were obtained using the PDFs from the HERAPDF analysis [14]. In practice, data for the reduced cross section, F2(x,Q2) – (y2/Y+)FL(x,Q2), were fitted, rather than F2 and FL separately.
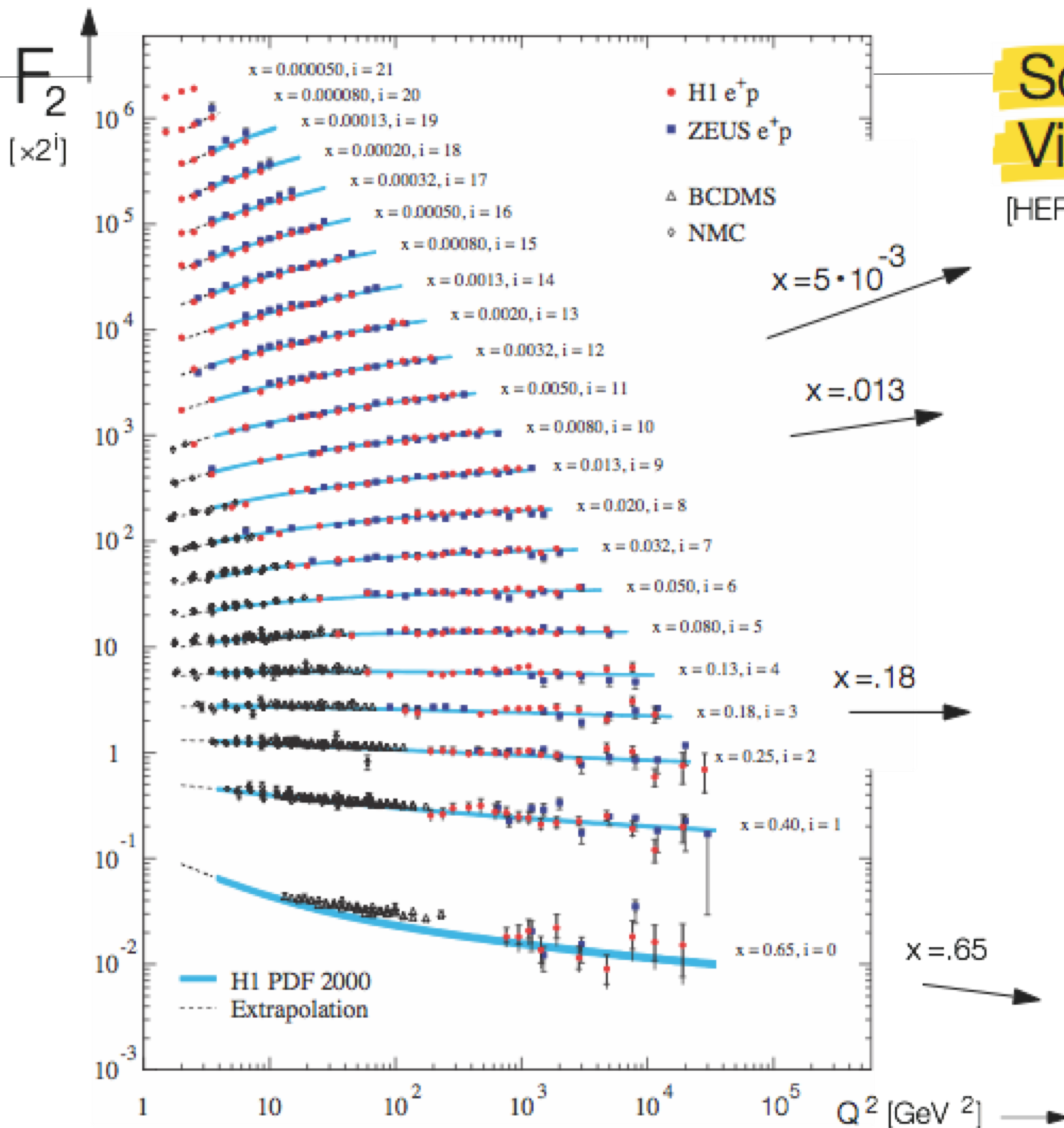
Scaling Behavior [SLAC 1972]

+ 6°   □ 18°
X 10°   △ 26°

$x = 0.25$

F_2 vs $Q^2 [GeV^2]$
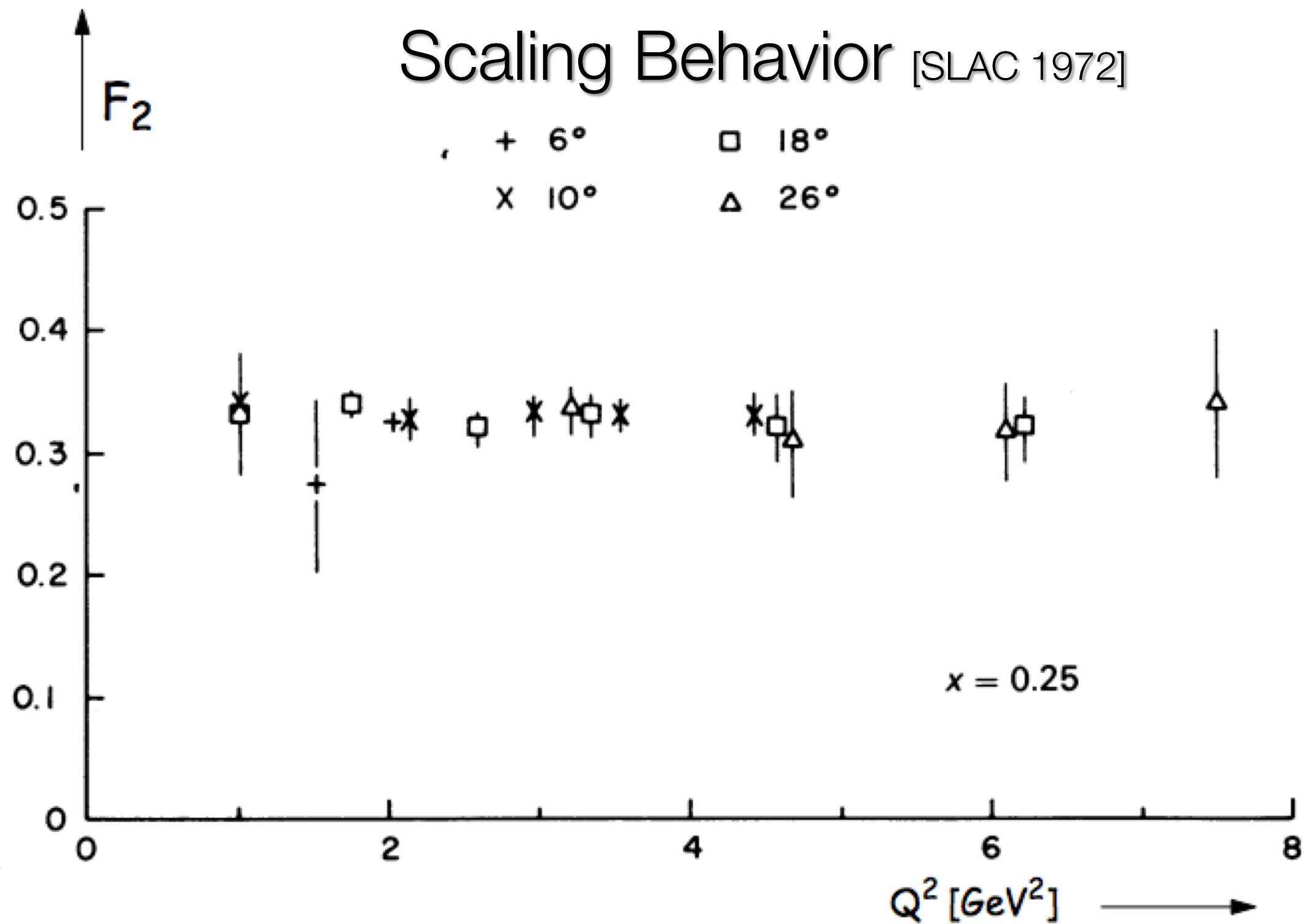
Scaling Violations [SLAC 1972]

$$F_2(x, Q^2) = \sum e_q^2 \, x q(x, Q^2)$$

Scaling Violations

[HERA & fixed target data]

$x = 5 \cdot 10^{-3}$

$x = .013$

Precision: 2-3%
[bulk region]

For $x < 10^{-2}$:
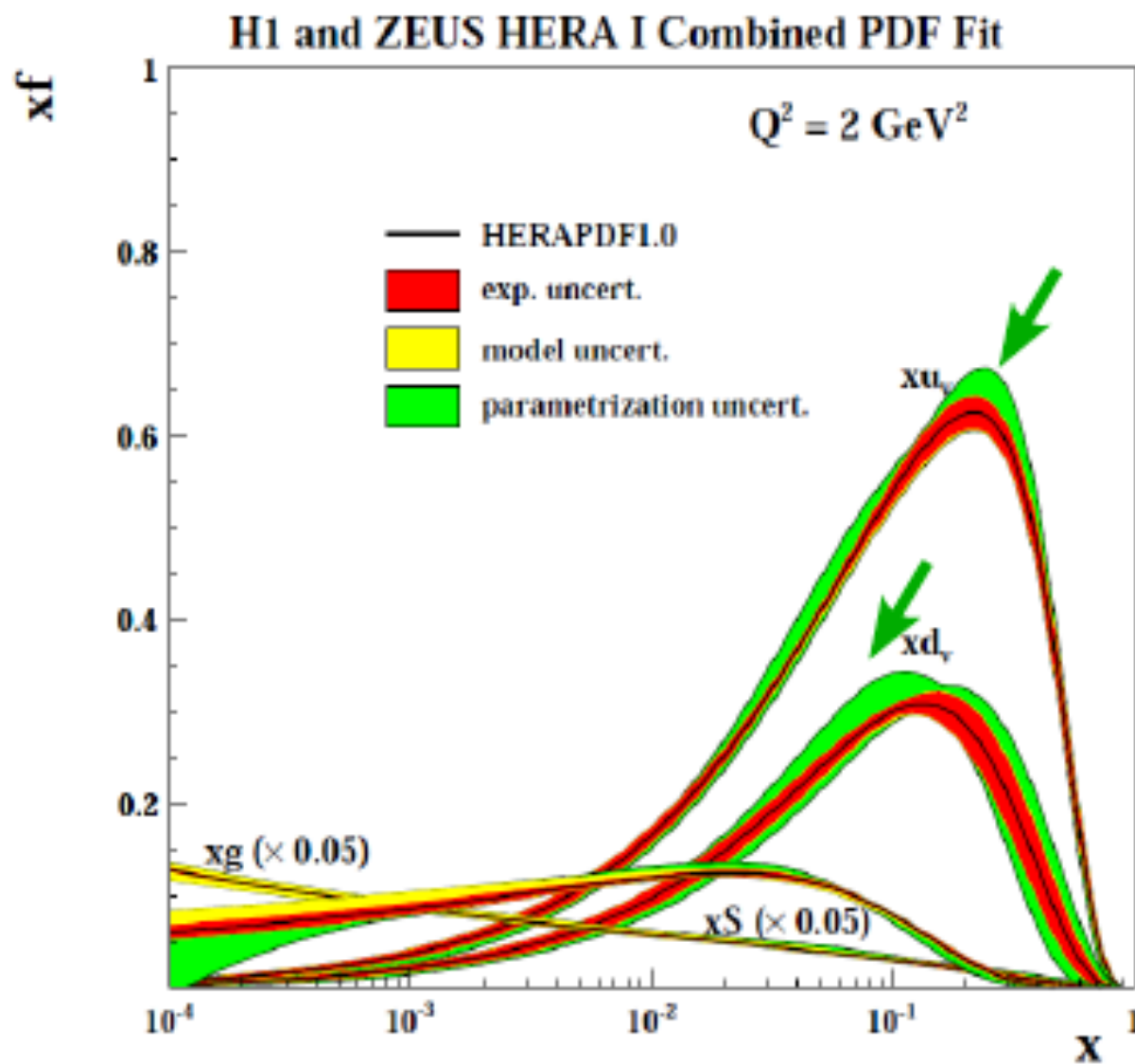
$$\frac{dF_2}{d\log Q^2} \sim g(x, Q^2) \cdot \alpha_s(Q^2)$$

$x = .18$

NLO QCD Fits:

Quark densities
Gluon density
Strong coupling α_s

$x = .65$

Hera

HERA I

H1 and ZEUS HERA I Combined PDF Fit

$Q^2 = 2 \text{ GeV}^2$

- — HERAPDF1.0
- exp. uncert.
- model uncert.
- parametrization uncert.

xu_v

xd_v

$xg \, (\times 0.05)$

$xS \, (\times 0.05)$

HERA I + II

H1 and ZEUS HERA I+II Combined PDF Fit

July 2010

$Q^2 = 2 \text{ GeV}^2$

- — HERAPDF1.5 (prel.)
- exp. uncert.
- model uncert.
- parametrization uncert.

xu_v

xd_v

$xg \, (\times 0.05)$

$xS \, (\times 0.05)$

HERA Structure Functions Working Group

Proton Parton Densities

H1 and ZEUS HERA I+II Combined PDF Fit

$Q^2 = 10\ GeV^2$

HERAPDF1.5 (prel.)
exp. uncert.
model uncert.
parametrization uncert.

xu_v

$xg\ (\times 0.05)$

xd_v

$xS\ (\times 0.05)$

H1 and ZEUS Combined PDF Fit

$Q^2 = 10\ GeV^2$

xg

xS

HERAPDF1.0 (HERA I)

HERAPDF1.5 (prel.)
(HERA I+II)

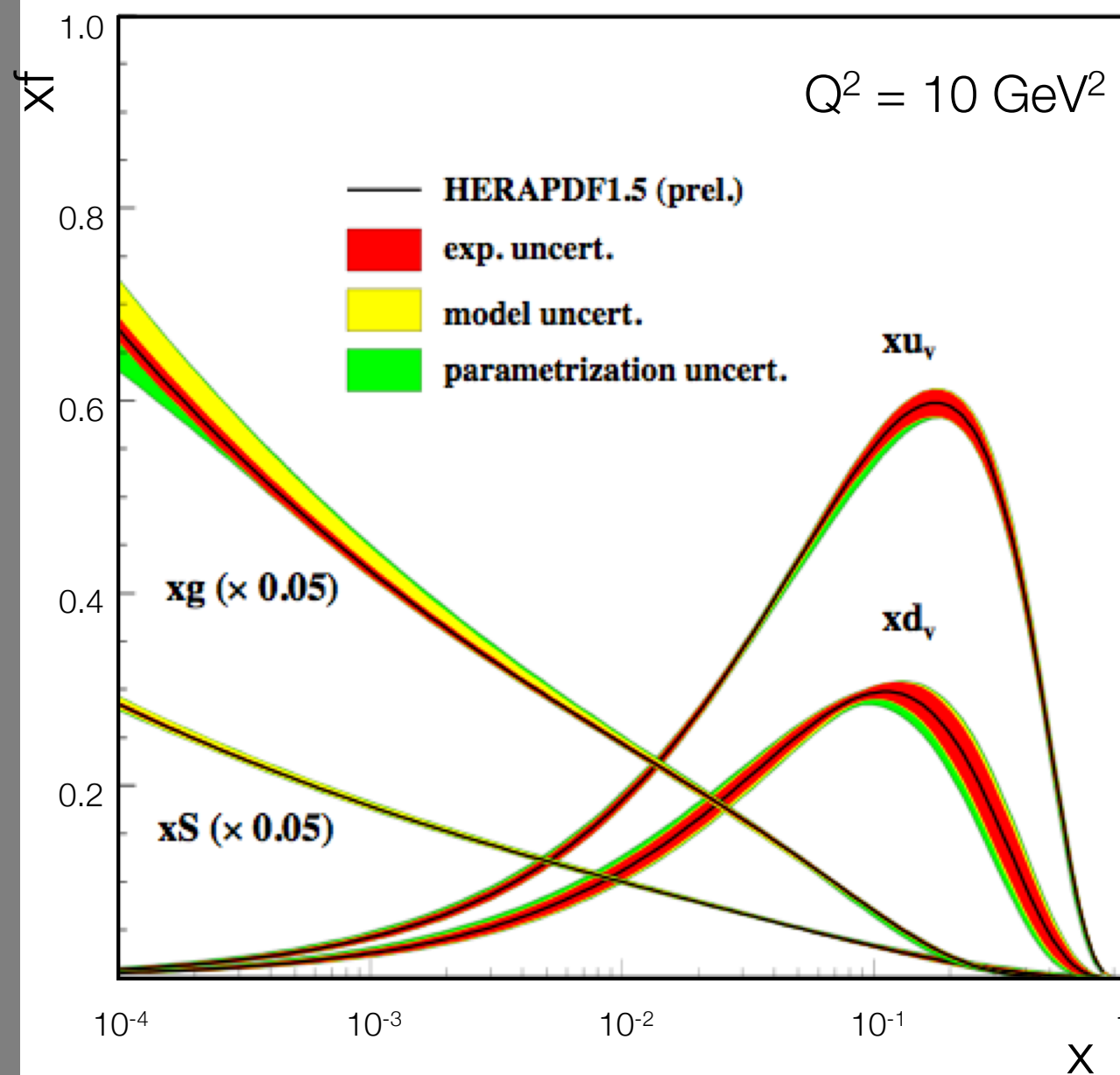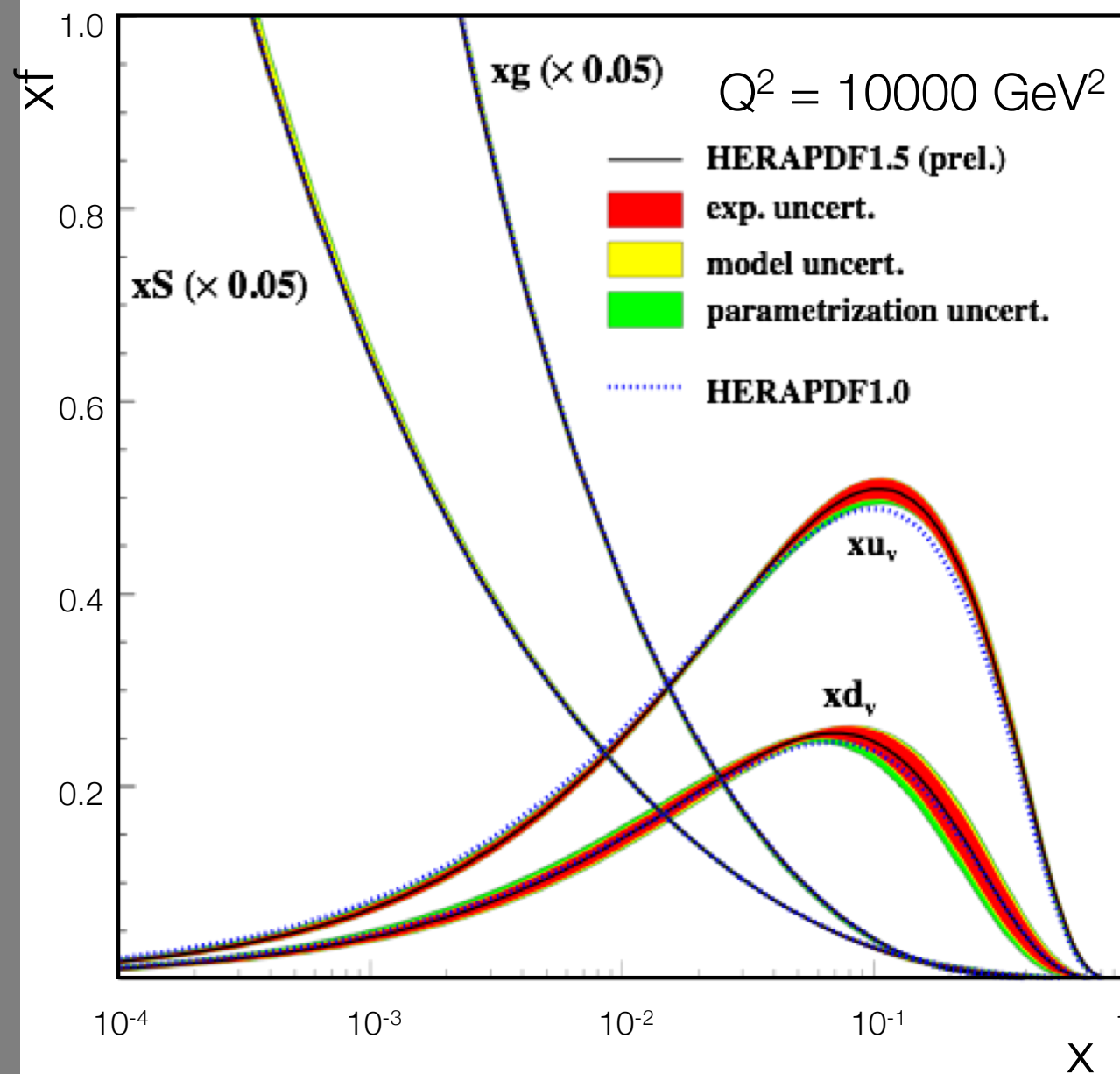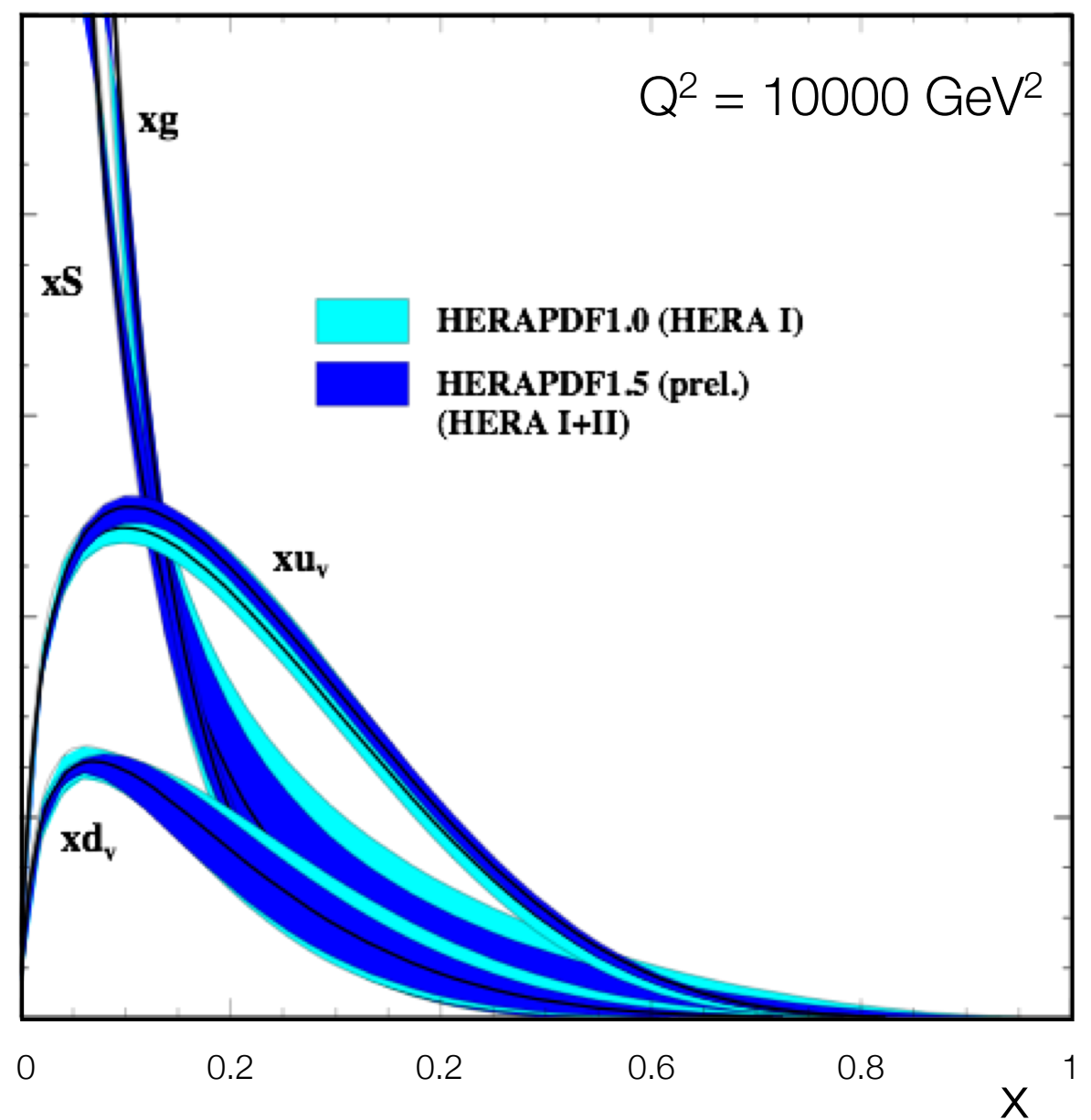xu_v

xd_v

HERA Structure Functions Working Group   July 2010

Proton Parton Densities

H1 and ZEUS HERA I+II Combined PDF Fit

H1 and ZEUS Combined PDF Fit

NNPDF2.3 NNLO N_F = 6

Gluon PDF

Gluons

Up quark PDF

Top PDF

- Gluon
- Up
- Charm
- Bottom
- Top
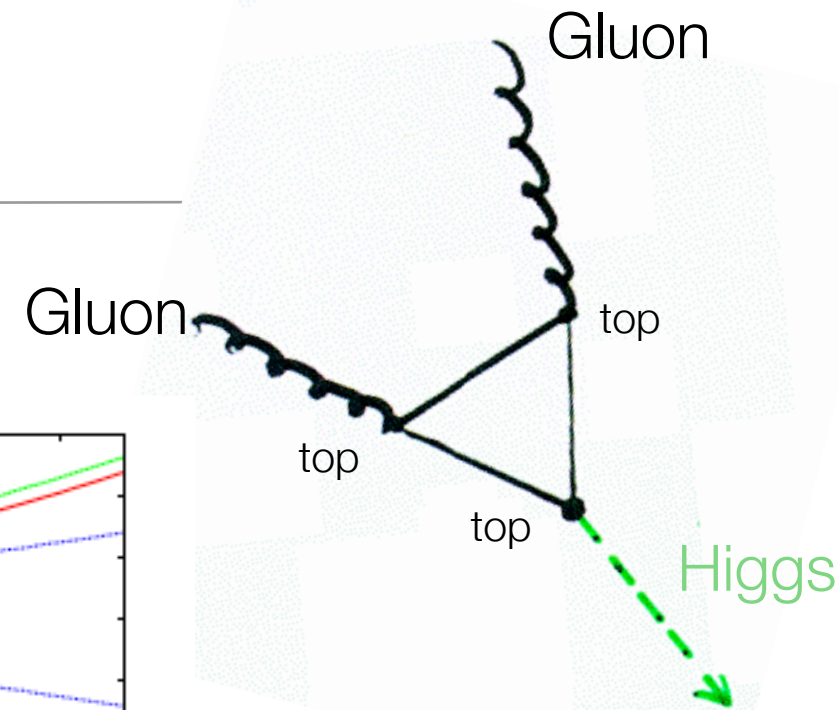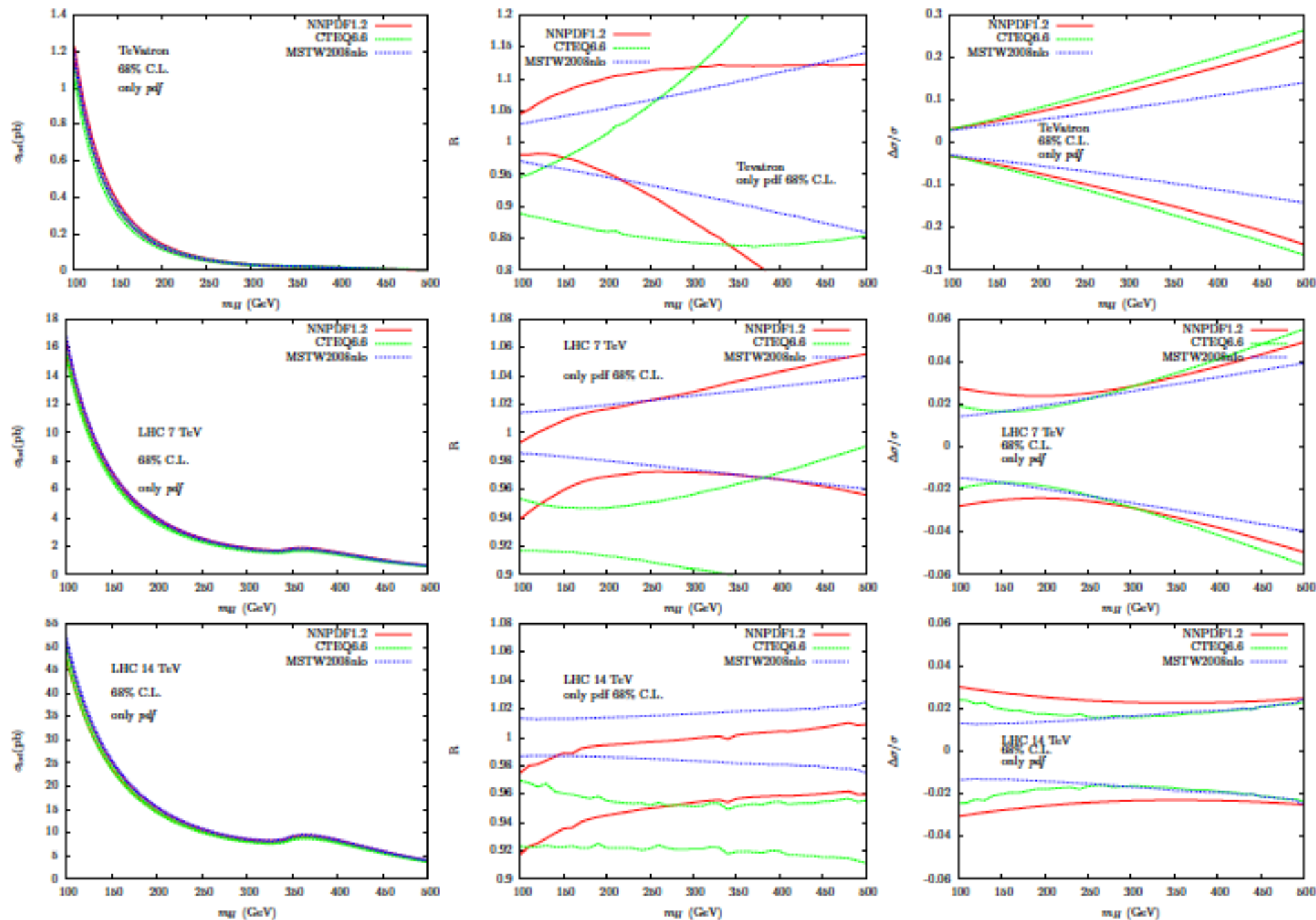
x PDF (x, Q^2 = 10 TeV)

x
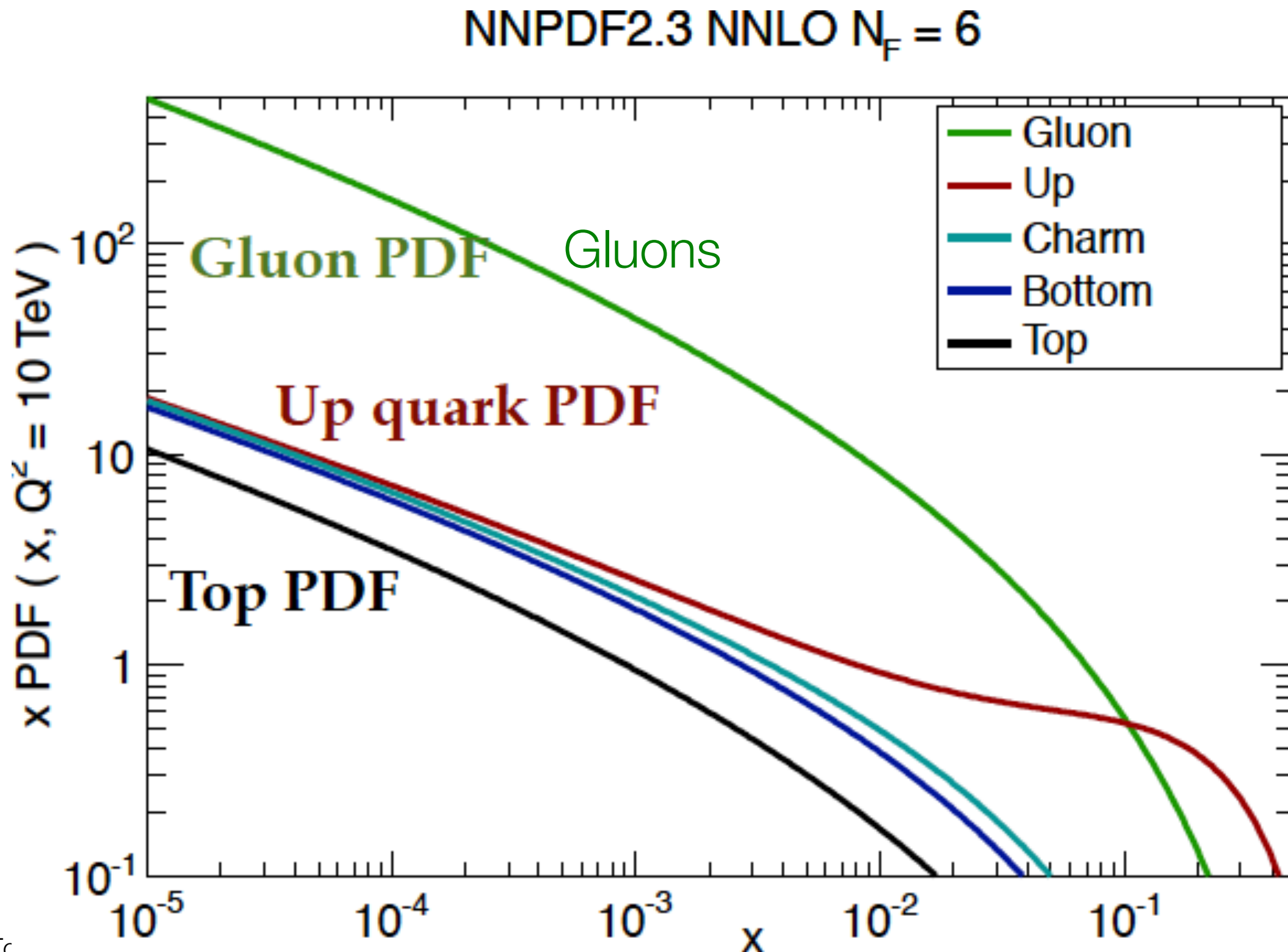
Measurement of parton functions

Table 19.1: The main processes relevant to global PDF analyses, ordered in three groups: fixed-target experiments, HERA and the $p\bar{p}$ Tevatron / pp LHC. For each process we give an indication of their dominant partonic subprocesses, the primary partons which are probed and the approximate range of x constrained by the data.

Fixed – target experiments

HERA & Tevatron

LHC

Process	Subprocess	Partons	x range
$\ell^{\pm}\{p,n\} \to \ell^{\pm} X$	$\gamma^* q \to q$	$q, \bar{q}, g$	$x \gtrsim 0.01$
$\ell^{\pm} n/p \to \ell^{\pm} X$	$\gamma^* d/u \to d/u$	d/u	$x \gtrsim 0.01$
$pp \to \mu^+ \mu^- X$	$u\bar{u}, d\bar{d} \to \gamma^*$	$\bar{q}$	$0.015 \lesssim x \lesssim 0.35$
$pn/pp \to \mu^+ \mu^- X$	$(u\bar{d})/(u\bar{u}) \to \gamma^*$	$\bar{d}/\bar{u}$	$0.015 \lesssim x \lesssim 0.35$
$\nu(\bar{\nu}) N \to \mu^-(\mu^+) X$	$W^* q \to q'$	$q, \bar{q}$	$0.01 \lesssim x \lesssim 0.5$
$\nu N \to \mu^- \mu^+ X$	$W^* s \to c$	s	$0.01 \lesssim x \lesssim 0.2$
$\bar{\nu} N \to \mu^+ \mu^- X$	$W^* \bar{s} \to \bar{c}$	$\bar{s}$	$0.01 \lesssim x \lesssim 0.2$
$e^{\pm} p \to e^{\pm} X$	$\gamma^* q \to q$	$g, q, \bar{q}$	$10^{-4} \lesssim x \lesssim 0.1$
$e^+ p \to \bar{\nu} X$	$W^+ \{d,s\} \to \{u,c\}$	d, s	$x \gtrsim 0.01$
$e^{\pm} p \to e^{\pm} c\bar{c} X, e^{\pm} b\bar{b} X$	$\gamma^* c \to c, \gamma^* g \to c\bar{c}$	c, b, g	$10^{-4} \lesssim x \lesssim 0.01$
$e^{\pm} p \to \text{jet} + X$	$\gamma^* g \to q\bar{q}$	g	$0.01 \lesssim x \lesssim 0.1$
$p\bar{p}, pp \to \text{jet} + X$	$gg, qg, qq \to 2j$	g, q	$0.00005 \lesssim x \lesssim 0.5$
$p\bar{p} \to (W^{\pm} \to \ell^{\pm}\nu) X$	$ud \to W^+, \bar{u}\bar{d} \to W^-$	$u, d, \bar{u}, \bar{d}$	$x \gtrsim 0.05$
$pp \to (W^{\pm} \to \ell^{\pm}\nu) X$	$u\bar{d} \to W^+, d\bar{u} \to W^-$	$u, d, \bar{u}, \bar{d}, g$	$x \gtrsim 0.001$
$p\bar{p}(pp) \to (Z \to \ell^+\ell^-) X$	$uu, dd, ..(u\bar{u}, ..) \to Z$	$u, d, ..(g)$	$x \gtrsim 0.001$
$pp \to W^- c, \ W^+ \bar{c}$	$gs \to W^- c$	$s, \bar{s}$	$x \sim 0.01$
$pp \to (\gamma^* \to \ell^+\ell^-) X$	$u\bar{u}, d\bar{d}, .. \to \gamma^*$	$\bar{q}, g$	$x \gtrsim 10^{-5}$
$pp \to (\gamma^* \to \ell^+\ell^-) X$	$u\gamma, d\gamma, .. \to \gamma^*$	γ	$x \gtrsim 10^{-2}$
$pp \to b\bar{b} X, \ t\bar{t} X$	$gg \to b\bar{b}, \ t\bar{t}$	g	$x \gtrsim 10^{-5}, 10^{-2}$
$pp \to \text{exclusive } J/\psi, \Upsilon$	$\gamma^*(gg) \to J/\psi, \Upsilon$	g	$x \gtrsim 10^{-5}, 10^{-4}$
$pp \to \gamma X$	$gq \to \gamma q, g\bar{q} \to \gamma\bar{q}$	g	$x \gtrsim 0.005$

Backup

Toni Baroncelli Experimental High Energy Physics at Colliders Winter 2019

Higgs Cross Section

The left column shows absolute results, the central column results normalized to the MSTW08 result, and the right column results normalized to each group's central result.
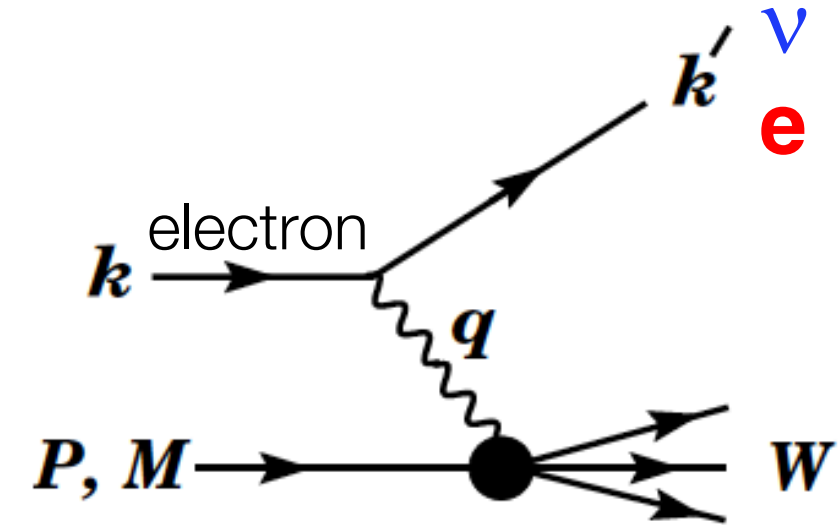
10 – 20 % PDF uncertainty

m_H

Physics at Hadron Colliders

ν

k′

e

electron

$k \longrightarrow$

q

$P, M \longrightarrow$

W

$$\eta_\gamma = 1 \quad ; \quad \eta_{\gamma Z} = \left(\frac{G_F M_Z^2}{2\sqrt{2}\pi\alpha}\right)\left(\frac{Q^2}{Q^2 + M_Z^2}\right) ;$$

$$\eta_Z = \eta_{\gamma Z}^2 \quad ; \quad \eta_W = \frac{1}{2}\left(\frac{G_F M_W^2}{4\pi\alpha}\frac{Q^2}{Q^2 + M_W^2}\right)^2 .$$

The cross sections for neutral- and charged-current deep inelastic scattering on unpolarized nucleons can be written in terms of the structure functions in the generic form

x = fraction of momentum carried by struck quark

y = fraction of lepton energy lost

$$\frac{d^2\sigma^i}{dxdy} = \frac{4\pi\alpha^2}{xyQ^2}\eta^i\left\{\left(1 - y - \frac{x^2y^2M^2}{Q^2}\right)F_2^i + y^2 x F_1^i \mp \left(y - \frac{y^2}{2}\right)xF_3^i\right\},$$

(19.8)

where $i = $ NC, CC corresponds to neutral-current $(eN \to eX)$ or charged-current $(eN \to \nu X$ or $\nu N \to eX)$ processes, respectively.

@ HERA